AD-A078 386

DEFENSE NUCLEAR AGENCY REACTION RATE HANDBOOK. SECOND EDITION. REVISION NUMBER 5, JUNE 1975

M. H. Bortner, et al

General Electric Company

Prepared for:

Defense Nuclear Agency

June 1975

DISTRIBUTED BY:

NTIS

National Technical Information Service
U. S. DEPARTMENT OF COMMERCE

DISCLAIMER NOTICE

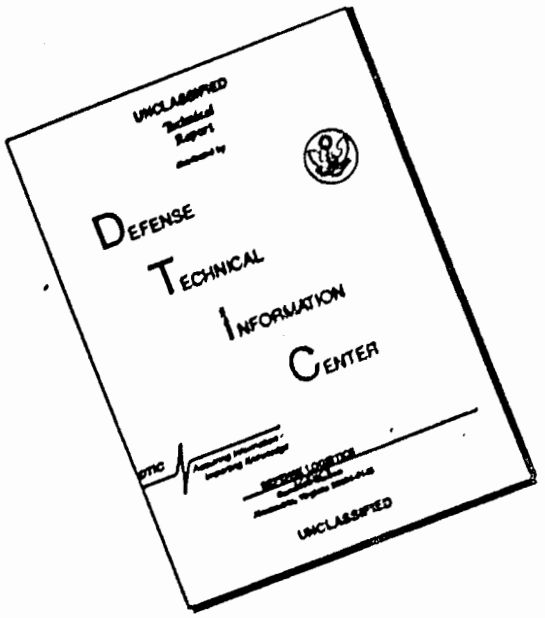

THIS DOCUMENT IS BEST QUALITY AVAILABLE. THE COPY FURNISHED TO DTIC CONTAINED A SIGNIFICANT NUMBER OF PAGES WHICH DO NOT REPRODUCE LEGIBLY.

AD A018386

351126

MEMORANDUM

To: All Recipients of the DNA Reaction Rate Handbook (DNA 1948H)

From: The Editors

Subject: Revision Number 5

Enclosed herewith you will find a copy of Revision Number 5 to the Handbook. It comprises a completely updated version of Chapter 18A and the brand-new Chapter 18B.

You should immediately discard the previous copy of Chapter 18A as well as the old pages 18B-1 and 18B-2, and place this new material in its proper order in your copy of the Handbook.

You should also enter on page iii in front of your Handbook the following information: Revision Number 5, Date of Issue: June 1975, Date of Receipt: whatever day you receive this, and sign your name in the last column.

We anticipate the issuance of Revision Number 6, updating Chapters 17, 19, and 20, later this spring, and Revision Number 7, revising the Appendices, by late summer.

DDC
RECEIVED
DEC 8 1975
D

Reproduced by
NATIONAL TECHNICAL
INFORMATION SERVICE
U.S. Department of Commerce
Springfield, VA 22151

DISTRIBUTION STATEMENT A
Approved for public release;
Distribution Unlimited

Copy No. _____

Revision No. 5, June 1975

DNA 1948H
(Formerly DASA 1948)

DEFENSE NUCLEAR AGENCY

REACTION RATE HANDBOOK
SECOND EDITION

Editors in Chief:
Dr. M.H. Bortner
Dr. T. Baurer

MARCH 1972

Project Officer Dr. C.A. Blank

APPROVED FOR PUBLIC RELEASE; DISTRIBUTION UNLIMITED

Organized by General Electric Space Sciences Laboratory
for Defense Nuclear Agency under Contracts
DASA 01 70 C 0082 and DASA 01 71 C 0145

D D C
DEC 8 1975

This effort supported by Defense Nuclear Agency
NWED Subtask Code HD028, Work Unit 11

Published by DASIAC
DoD Nuclear Information and Analysis Center
General Electric Company TEMPO
Santa Barbara, California

18. ION-NEUTRAL REACTIONS
A. THERMAL PROCESSES

Eldon E. Ferguson
Aeronomy Laboratory
National Oceanic and Atmospheric Administration
Research Laboratories
(Latest Revision 25 February 1975).

18A.1 INTRODUCTION

Progress in the field of ion-neutral reactions has been very rapid in the few years since the first edition of the Reaction Rate Handbook was prepared. The number of atmospherically relevant rate constants known has multiplied greatly and most of those previously known have been improved so that an almost complete rewriting of this chapter (prepared by Wade L. Fite in the first edition of the Handbook) was called for. The convenient format of Fite is retained. The emphasis of this chapter is on data tabulation. The reactions reported are positive- and negative-ion charge-transfer (electron transfer) with neutrals, ion-atom-interchange reactions (chemical rearrangement), and three-body association reactions. Associative-detachment reactions of negative ions are covered in Chapter 17. The survey is restricted largely to low (near-thermal) energies.

Some useful general references and review articles are:

(a) Sinnott, G.A., Bibliography of Ion-Molecule Reaction Rate Data, JILA Information Center Report No. 9, University of Colorado, Boulder, Colorado (1969).

(b) McDaniel, E.W., V. Cermak, A. Dalgarno, E.E. Ferguson, and L. Friedman, Ion-Molecule Reactions, John Wiley, New York (1970).

(c) Hochstim, A.R., Ed., Bibliography of Chemical Kinetics and Collision Processes, Plenum Press, New York (1969).

(d) Franklin, J.L., J.G. Dillard, H.M. Rosenstock, J.T. Herron, K. Draxl, and F.H. Field, Ionization Potentials, Appearance Potentials, and Heats of Formation of Gaseous Ions, NSRDS-NBS 26, U.S. Gov't. Printing Office, Washington (1969).

(e) Schiff, H.I., Ed., Proceedings of the Symposium on Laboratory Measurements of Aeronomic Interest, Can. J. Chem. 47, No. 10 (1969).

(f) Ferguson, E.E., Ann. Geophys. 26, 851 (1970).

(g) Ferguson, E.E., Ann. Geophys. 26, 857 (1970).

(h) Franklin, J.L., Ed., Ion-Molecule Reactions, 2 Volumes, Plenum Press, New York (1972).

(i) Ferguson, E.E., Accts. Chem. Res. 3, 402 (1970).

(j) Ferguson E.E., Laboratory Measurements of D-Region Ion-Molecule Reactions, in Upper Atmospheric Models and Related experiments, G. Fiocco, Ed., Reidel, Dordrecht, Holland (1971).

(k) Ferguson, E.E., Ann. Geophys. 28, 387 (1972).

(l) Ferguson, E.E., Revs. Geophys. Space Phys. 12, 703 (1974).

18A.2 TECHNIQUES

The experimental techniques in use are described in detail in Chapter 7, in reference item (j) above, and elsewhere. Only brief reference is made here to recent advances which have led to new reaction-rate data.

18A.2.1 Stationary Afterglows

The use of stationary afterglows for ion-neutral reaction studies is described in Chapter 7. Important studies (Reference 18A-1) in the complex nitric oxide system have been carried out with and without added water vapor, looking at both positive- and negative-ion processes. Other work (References 18A-2, 18A-3) has concentrated on the ionospheric reactions, varying the gas temperature from 185 to 700 K in some cases.

18A.2.2 Flowing Afterglow

The flowing-afterglow technique, a versatile method for ion-neutral reaction studies in the sense of being applicable to a wide range of ion and neutral reactants, has been extended to cover the temperature range 80-600 K for some reactions (References 18A-4, 18A-5). It has been applied to metal-ion reactions (Reference 18A-6) and to three-body ion reactions (References 18A-7 through 18A-9). The method has been applied to measurements of atmospheric-ion charge-transfer with sodium (Reference 18A-10) and ion reactions with water (References 18A-11 through 18A-13). The NOAA system

discussed in Chapter 7 has been extended to study O^- and O_2^- reactions with electronically excited $O_2(a^1\Delta_g)$ (Reference 18A-16), and to study ion-pair states formed by an ion-neutral reaction spectroscopically in the charge transfer of He^+ with O_2 (Reference 18A-17).

18A.2.3 Secondary Ions in Mass Spectrometers

The mass-spectrometer ions-source technique, long the standard tool for radiation chemistry, has made important contributions to ionospheric reaction-rate data. The photoionization source method of Harteck (References 18A-18, 18A-19) has allowed the measurement of a large number of ionospheric reactions, generally corroborating earlier afterglow results. The isotope studies of Paulson (Reference 18A-15) have allowed some mechanisms of ionospheric reactions to be determined. In addition Paulson has obtained data on the energy dependence of certain reactions, and has also extended the mass spectrometer to the study of ionospheric negative ions (Reference 18A-15). Lenarle (References 18A-20, 18A-21) has made important measurements of two- and three-body reactions involving water, which are difficult to do otherwise. Lenarle and also Conway have measured equilibrium constants in high-pressure mass-spectrometer ion sources, adding greatly to our knowledge of the important ionospheric-ion chemistry.

18A.2.4 Crossed-Beam Experiments

The method of Lerner and Rutherford (cf. Chapter 7) continues to produce large amounts of valuable ionospheric information on charge-transfer processes, both for positive and negative ions, at energies of many electron volts (Reference 18A-22). The relative constancy of ion-transfer rate constants from thermal levels to several electron volts allows a reasonable extrapolation of the low-energy ion-beam data in many cases. Important data on the reactions of excited-state ions, which are almost unavailable by any other technique, have also been obtained (Reference 18A-23). The crossed-beam studies have shown great versatility in the kinds of reactions studied.

18A.2.5 Drift-Tube Techniques

A very promising new development is the use of drift tubes to study ionospheric ion-neutral reactions over a range of energies, from thermal levels to several electron volts, not otherwise readily accessible. The works of Biondi (References 18A-24, 18A-25),

Varney (Reference 18A-26), Hasted (References 18A-27, 18A-28), McDaniel (Reference 18A-29), and Kaneko (Reference 18A-30) are especially noteworthy.

18A.3 EXAMPLES OF IMPORTANT IONOSPHERIC REACTIONS

Several of the more important ionospheric reactions are discussed in some detail in this section. A variety of different types of reactions are discussed in order to point out different kinds of problems which arise. Reviews are available by Fite (Reference 18A-31) for aeronomic positive-ion reactions, and by Ferguson (Reference 18A-32) for aeronomic negative-ion reactions.

18A.3.1 $He^+ + N_2 \rightarrow N^+ + N + He$
$\rightarrow N_2^+ + He$

This is an example of one of the simplest ionospheric reactions to be measured, involving an ion of a stable neutral reacting with a stable neutral. Consequently a number of measurements in a variety of experiments support a value $k = (1.2 \pm 0.3) \times 10^{-9}$ cm^3 sec. The rate constant is insensitive to temperature variation and to vibrational excitation of the nitrogen. The branching ratio, i.e., $N^+ : N_2^+$ product ratio, is less certain than the rate-constant measurement, since it involves a knowledge of the sampling efficiency as a function of mass for the mass spectrometer, which is unnecessary for the rate-constant measurement alone in certain techniques. The $N^+ : N_2^+$ ratio lies between one and two, and depends on the nitrogen vibrational temperature. This reaction is near resonant charge transfer into the $N^+(^1D)$ state, which then radiates the second-negative system to give ground-state N_2^+, or predissociates to give N^+ (Reference 18A-10). This is one of the few reactions for which the product states are well known. There is evidence that the N_2^+ produced is rotationally excited.

18A.3.2 $O^+ + O_2 \rightarrow O_2^+ + O$

This reaction has been measured by several workers; all results are consistent with $k = 2.0 \times 10^{-11} (T/300)^{-1/2}$ cm^3 sec for the temperature range 80-1000 K (References 18A-3 through 18A-9). Recent data on the energy dependence are presented by McFarland et al (Reference 18A-33).

18A.3.3 $O^+ + N_2 \rightarrow NO^+ + N$

This reaction has been studied in great detail, often with conflicting results. The rate constant is 1.2×10^{-12} cm^3 sec at 300 K, and decreases to about 5×10^{-13} cm^3 sec at 600 K (Reference 18A-4). The reaction-rate constant is extremely sensitive to the nitrogen vibrational temperature, increasing sharply for $T_{vib} > 1200$ K (Reference 18A-34). At higher energies, where the ion kinetic energy exceeds [illegible] eV, the rate constant also increases sharply. It seems likely that in the important ionospheric temperature range 600-2[illegible] K the effect of nitrogen vibrational-temperature increase will dominate the effect of kinetic-energy increase. Fahey et al (Reference 18A-35) have obtained cross-section data for ion kinetic energies from thermal levels to about one electron volt. C. Mulley has developed a theory for this reaction which yields some extrapolation tables (Reference 18A-36). McFarland et al have recently provided expressions for the energy dependence (Reference 18A-33).

18A.3.4 $N_2^+ + O_2 \rightarrow O_2^+ + N_2$

Johnsen et al (Reference 18A-2) find the rate constant to be about 5×10^{-11} cm^3 sec at [illegible] K and to decrease regularly to about 10^{-11} cm^3 sec at ion kinetic energy equal to one electron volt. This agrees very well with the drift-tube data (Reference 18A-4) in the region of overlap, 300 K. A more comprehensive expression for the energy dependence has recently been provided by McFarland et al (Reference 18A-33).

18.3.5 $SiO^+ + O \rightarrow Si^+ + O_2$

This reaction has been found to have a rate constant of approximately 2×10^{-10} cm^3 sec (Reference 18A-37). A reaction such as this is very difficult to measure, since the reactant ion is not readily produced, and since the neutral reactant is unstable. No experimental data exist in which the temperature dependence of reactions involving unstable neutrals are measured.

18.3.6 $Mg^+ + O_3 \rightarrow MgO^+ + O_2$

This reaction has a rate constant equal to 2.5×10^{-9} cm^3 sec (Reference 18A-38), and represents a kind of reaction which is difficult to measure because of problems in handling both the ion and neutral reactants. The measurements are correspondingly less accurate than for experimentally simpler reactions, and such details as the energy dependence of the rate constant are not available.

18A.3.7 $O_2^+ + Na \rightarrow Na^+ + O_2$

This reaction and the analogous N_2^+ and NO^+ charge-transfer reactions have been measured in a flowing-afterglow system (Reference 18A-10), the rate constant for the O_2^+ reaction being 6.7×10^{-10} cm^3/sec at 300 K. Reactions of ions with neutral metals pose problems in measurement because of the difficulty of handling and measuring the neutral reactant. However, such reactions are being treated in crossed-beam experiments, down to a few electron volts of ion energy (see Table 18A-6). Because of the difficulties enumerated above, crossed-beam measurements will probably supply the bulk of useful information of this kind for some years. In the case of charge-transfer reactions generally, the rate-constant dependence on energy is usually relatively slight, so that the long extrapolation from a few electron volts to atmospheric temperatures is not so hazardous as would be the case for ion-atom interchange. However, for $O_2^+ + Na$ the extrapolation gives about twice as large a rate constant as the flowing-afterglow measurement, and for $N_2^+ + Na$ the discrepancy is a factor of four, the extrapolated beam result again being larger. An important detail about reactions such as this which remains undetermined is the chemical state of the products, i.e., either O_2 or $O + O$ could be produced in the present instance.

18A.3.8 $O_2^+ + O_2 + M \rightarrow O_4^+ + M$

This reaction is particularly important with respect to the D-region chemistry (Reference 18A-37). Reactions such as this one are difficult to measure in the laboratory and good rate data are correspondingly sparse. The problem is compounded by the fact that several third bodies (M) are of potential importance in the atmosphere, and by the additional fact that three-body rate constants are markedly temperature-dependent. Much of the atmospheric interest is in the D-region where $T < 300$ K, which is not a readily accessible range in most laboratory experiments. For M $= O_2$ and T $= 298$ K, Durden et al (Reference 18A-20) find $k = 2.8 \times 10^{-30}$ cm^6/sec for the above reaction. For M $=$ He and T $= 80$ K, Bohme et al (Reference 18A-8) find $k = 3.1 \times 10^{-29}$ cm^6/sec. This illustrates the marked increase in rate constant with decreasing temperature, a very general finding. It is unlikely that helium is as effective a third body as molecular oxygen at any temperature. In the analogous N_2^+ reaction at 300 K, molecular nitrogen is 2.5 times as effective as helium, for example (Reference 18A-8). This reaction ($N_2^+ + 2N_2 \rightarrow N_4^+ + N_2$) is about 18 times faster than the corresponding O_2^+ reaction cited above.

which is attributable to a larger N_4^+ dissociation energy. Three-body-association rate constants are expected to increase markedly, both with the dissociation energy of the complex formed and with the sizes of the molecules involved, as well as with a decrease in temperature.

18A.3.9 $O_2^- \cdot O_2 \cdot M \rightarrow O_4^- \cdot M$

It is recognized that O_4^- formation may be of great importance in D-region negative-ion chemistry (Reference 18A-38), owing to a number of rapid O_4^- reactions, e.g., $O_4^- + NO \rightarrow NO_3^- + O_2$, which lead to stable (non-electron-detaching) products. This reaction appears to be quite slow; McKnight and Sawina (Reference 18A-39) report $k = 4 \times 10^{-31}$ cm^6 sec^{-1} at 310 K, from drift-tube studies. This is an order of magnitude slower than the analogous O_2^+ positive-ion association at room temperature, suggesting a definite anomaly inasmuch as the O_4^- dissociation energy is thought to be greater (0.59 eV) than the O_4^+ bond energy (0.42 eV).

18A.3.10 $NO_2^- \cdot NO_2 \rightarrow NO_3^- \cdot NO$

This reaction is observed to take place with a rate constant of approximately 4×10^{-12} cm^3 sec^{-1} (Reference 18A-38), indicating that $EA(NO_3) > EA(O_2) + 0.1$ eV, or that $EA(NO_3) > 2.7$ eV at least, and probably > 3.1 eV. Additionally, these data seem to establish that the reverse reaction $NO_3^- + NO$ is endothermic. However, it has also been found (Reference 18A-40) that a form of NO_3^- can be produced which reacts readily with NO in the laboratory. Presumably this NO_3 is a different stable geometrical form of the same empirical formula NO_3^-. Polyatomic ions are known to exist in different isomeric forms, e.g., O-N-O-O$^-$ and O-$\overset{\displaystyle O}{\underset{\displaystyle O}{\overset{|}{\underset{|}{C}}}}$-O$^-$ in the present instance. This suggests a potential source of error in certain laboratory observations, as well as a considerable additional complexity in the D-region chemistry, where such factors may have an important influence upon the ion chemistry in particular. The electron affinity of NO_2 has been determined to be 2.38 ± 0.05 eV (Reference 18A-41) and that of NO_3 has been determined to be 3.9 ± 0.2 eV (Reference 18A-42).

18A.3.11 The $O_2^+ - H_2O$ Sequence

A reaction scheme which proceeds sequentially from O_2^+ to $H_3O^+ \cdot H_2O$ and higher hydrated clusters, is known to be very

significant in the D-region. The three-body association of O_2^+ to O_4^+, discussed in subsection 18A.3.8, is efficient at approximately 200 K in the D-region. Following this initial step, the sequence proceeds via:

(a) $O_4^+ + H_2O \rightarrow O_2^+ \cdot H_2O + O_2$	1.4×10^{-9}	2.2×10^{-9}	1.5×10^{-9}
(b) $O_2^+ \cdot H_2O + H_2O \rightarrow H_3O^+ \cdot OH + O_2$	9×10^{-10}	1.5×10^{-9}	1.0×10^{-9}
(c) $\rightarrow H_3O^+ + OH + O_2$	3×10^{-10}	$\leq 1.0 \times 10^{-10}$	2×10^{-10}
(d) $H_3O^+ \cdot OH + H_2O \rightarrow H_3O^+ \cdot H_2O + OH$	$\geq 1 \times 10^{-9}$	3.2×10^{-9}	1.4×10^{-9}

These are followed in turn by further three-body clustering of water molecules to the hydrated cluster-ions. Reaction (c) (producing H_3O^+) is almost certainly endothermic and presumably occurs as a consequence of vibrational excitation of the reactant $O_2^+ \cdot H_2O$. This may account for reported variations in the branching ratio represented by reactions (b) and (c), with different experimental conditions. Fehsenfeld (Reference 18A-41) has found that the reaction:

(e) $O_4^+ + O \rightarrow O_2^+ + O_3$

has a large rate constant, i.e., $k = (3 \pm 2) \times 10^{-10}$ cm^3/sec. This plays an important role in the $O_2^+ - H_2O$ reaction scheme in the D-region.

In addition to $O_2^+ \cdot H_2O$ production from O_4^+, direct O_2^+ hydration can occur:

(f) $O_2^+ + H_2O + M \rightarrow O_2^+ \cdot H_2O + M$.

Howard et al have found the rate constant to be 2.3×10^{-28} cm^6/sec for $M = O_2$ at 296 K (Reference 18A-13), and Good et al (Reference 18A-21) and Fehsenfeld et al (Reference 18A-9) have obtained similar results.

---

[a] Rate constants from Kebarle (Reference 18A-21), in cm^3/sec.
[b] Rate constants from Fehsenfeld (Reference 18A-9), in cm^3/sec.
[c] Rate constants from Howard (Reference 18A-13), in cm^3 sec.

18A.3.12 The $NO^+ - H_2O$ Sequence

The sequence of events involved in NO^+ hydration in the D-region has been shown (References 18A-1, 18A-12, 18A-37, 18A-43, 18A-44) to include:

		F	H	P	
(a) $NO^+ + H_2O + M \rightarrow NO^+ \cdot H_2O + M$.	$k =$	1.6×10^{-28}	1.4×10^{-28}	1.6×10^{-28}	$cm^6/sec.$
(b) $NO^+ \cdot H_2O + H_2O + M \rightleftarrows NO^+(H_2O)_2 + M$.	$k =$	1.0×10^{-27}	1.2×10^{-27}	1.1×10^{-27}	$cm^6/sec.$
	$k_r =$	$< 1 \times 10^{-13}$	1.7×10^{-14}	1.4×10^{-14}	$cm^3/sec.$
(c) $NO^+(H_2O)_2 + H_2O + M \rightleftarrows NO^+(H_2O)_3 + M$.	$k =$	2.0×10^{-27}	1.4×10^{-27}	1.9×10^{-27}	$cm^6/sec.$
	$k_r =$	1.3×10^{-12}	1.4×10^{-12}	1.9×10^{-12}	$cm^3/sec.$
(d) $NO^+(H_2O)_3 + H_2O \rightarrow H_3O^+(H_2O)_2 + HNO_2$	$k =$	8×10^{-11}	7×10^{-11}	7×10^{-11}	$cm^3/sec.$

The results presented above agree remarkably well in view of the complexity of the coupled reaction sequence.

18A.3.13 $NO_2^+ + NO \rightarrow NO^+ + NO_2$

This reaction has been found to be very rapid; $k = 2.9 \times 10^{-10}$ cm^3/sec (Reference 18A-45), which is important insofar as it confirms that $IP(NO_2) > IP(NO)$.

18A.3.14 $NO^+ + CO_2 + M \rightarrow NO^+ \cdot CO_2 + M$

The reaction, where $M = N_2$, has been found to have a rate constant of 3×10^{-29} cm^6/sec at 197 K in the afterglow (Reference 18A-46). Furthermore, the reaction $NO^+ \cdot CO_2 + H_2O \rightarrow NO^+ \cdot H_2O + CO_2$ is very fast, i.e., $k \sim 10^{-9}$ cm^3/sec. These combined results are important in that the CO_2 association with NO^+, followed by the

---

Rate constants under "F" (via flowing afterglow, where $M = N_2$) are from Fehsenfeld et al (Reference 18A-43), who also report data for M = He, Ar. Rate constants under "H" (via flowing afterglow, where $M = N_2$) are from Howard et al (Reference 18A-12), who also report data for M = He, Ar, O_2. Rate constants under "P" (via stationary afterglow, where M = NO) are from Puckett and Teague (Reference 18A-44). All data pertain to room-temperature measurements.

rapid "switching" of CO_2 and H_2C, appears to be a more rapid means of hydrating NO^+ in the D-region than the direct three-body association of NO^+ and H_2O.

18A.4 SUMMARY OF REACTION RATE CONSTANTS

Following are several tables of reaction-rate constants of atmospheric interest: Table 18A-1, positive-ion charge-transfer reactions; Table 18A-2, negative-ion charge-transfer reactions; Table 18A-3, positive-ion atom-interchange reactions: Table 18A-4, negative-ion atom-interchange reactions; Table 18A-5, three-body positive-ion reactions; Table 18A-6, three-body negative-ion reactions; and Table 18A-7, the Gulf General Atomic charge-transfer reactions of positive ions with metallic neutrals. The latter are kept separate because they form a cohesive set of data and because of the special extrapolation methods used to estimate the thermal-energy rate constants. Throughout all tables except the last (18A-7), the rate constants are reported in the form m(-n), which designates $m \times 10^{-n}$.

Unless otherwise specified, rate constants were obtained at room temperature. For some older measurements, review papers are referenced rather than the original papers.

Table 18A-1. Pasitive-ian charge-transfer.

Reaction	k (cm^3/sec)	References	Comments
1.a. $He^+ + N_2 \rightarrow He + N + N^+$	1.2(-9)	18A-31, 47 48	See par. 18A.3.1.
b. $\rightarrow He + N_2^+$			
2. $He^+ + O_2 \rightarrow He + O + O^+$	1.1(-9)	18A-31, 47	Also produces O_2^+.
3. $He_2^+ + N_2 \rightarrow 2He + N_2^+$	1.2(-9)	18A-48, 49	200-900K
4. $O^+ + H \rightarrow O + H^+$	6.8(-10)	18A-50, 51	σ = 20-40 A^2
5.* $O^+ + O_2 \rightarrow O + O_2^+$	2.0(-11)	18A-3,4, 33	See par. 18A.3.2.
6. $O^+ + NO \rightarrow O + NO^+$	~ 8(-13)	18A-52	300K; k increases to ~ 1 (-11) at 1 eV relative ion kinetic energy.
7. $O^+ + NO_2 \rightarrow NO_2^+ + O$	1.6(-9)	18A-53	393K
8. $O^+ + N_2O \rightarrow N_2O^+ + O$	2.2(-10)	18A-54	Cf. Table 18A-3, Reaction 2.
9. $O^+ + H_2O \rightarrow H_2O^+ + O$	2.33(-9)	18A-11	
10.* $N^+ + O_2 \rightarrow N + O_2^+$	5.5(-10)	18A-4, 25, 33	Cf. Table 18A-3, Reaction 5

* Recent data on the energy dependences of these reactions are collected in Reference 18A-33.

Table 18A-1. (Cont'd)

Reaction	k (cm^3/sec)	References	Comments
11. $N^+ + NO \rightarrow N + NO^+$	8.0(-10)	18A-55	
12. $N^+ + H_2O \rightarrow H_2O^+ + N$	2.57(-9)	18A-11	
13. $O_2^+(a^4\Pi_u) + O_2 \rightarrow O_2 + O_2^+$	3(-10)	18A-56	Quenching reaction.
14. $O_2^+(a^4\Pi_u) + N_2 \rightarrow N_2^+ + O_2$	4.0(-10)	18A-56	
15.a. $O_2^+(X^2\Pi_g) + NO \rightarrow O_2 + NO^+$	4.4(-10)	18A-57	*
b. $O_2^+(a^4\Pi_u) + NO \rightarrow O_2 + NO^+$	1.1(-9)	18A-57	*
16. $O_2^+ + NO_2 \rightarrow NO_2^+ + O_2$	6.6(-10)	18A-59	
17. $O_2^+ + Na \rightarrow O_2 + Na^+$	6.7(-10)	18A-10	See par. 18A.3.7. Cf. Table 18A-3, Reaction 10.
18. $N_2^+ + O \rightarrow N_2 + O^+$	1.0(-11)	18A-60	**
19. $N_2^+ + N \rightarrow N_2 + N^+$	<1.0(-11)	18A-61	Not observed.

* k for the ground-state reaction (15.a.) was formerly cited as 6.3(-10), based on the inadvertent experimental admixture of the excited-state reaction (15.b.) (References 18A-25, 18A-58).

** 300K; almost independent of temperature. Branching ratio favors Reaction 11, Table 18A-3 over this by 0.93/0.07.

Table 18A-1. (Cont'd)

Reaction	k (cm^3/sec)	References	Comments
20.* $N_2^+ + O_2 \rightarrow N_2 + O_2^+$	5.0(-11)	18A-25, 31, 33, 47	See par. 18A.3.4.
21. $N_2^+ + NO \rightarrow N_2 + NO^+$	3.3(-10)	18A-58	
22.a. $N_2^+ + H_2O \rightarrow H_2O^+ + N_2$	2.19(-9)	18A-11	
b. $\rightarrow N_2H^+ + OH$			
23. $N_2^+ + Na \rightarrow N_2 + Na^+$	5.8(-10)	18A-10	N_2 may dissociate
24. $N_4^+ + O_2 \rightarrow O_2^+ + 2N_2$	4(-10)	18A-46	
25. $NO^+ + Na \rightarrow NO + Na^+$	7.0(-11)	18A-10	
26. $NO_2^+ + NO \rightarrow NO_2 + NO^+$	2.9(-10)	18A-45	See par. 18A.3.12.
27. $H^+ + O \rightarrow O^+ + H$	3.8(-10)	18A-51	
28. $H^+ + NO \rightarrow NO^+ + H$	1.9(-9)	18A-51	
29. $OH^+ + O_2 \rightarrow OH + O_2^+$	~2.0(-10)	18A-62	

* Recent data on the energy dependence of this reaction are collected in Reference 18A-33.

Table 18A-1. (Cont'd.)

Reaction	k (cm^3/sec)	References	Comments
30. $H_2O^+ + O_2 \rightarrow H_2O + O_2^+$	~2.0(-10)	18A-47, 62	
31. $CO^+ + O \rightarrow O^+ + CO$	1.4(-10)	18A-51	
32. $CO^+ + NO \rightarrow NO^+ + CO$	3.3(-10)	18A-51	
33. $CO_2^+ + O \rightarrow CO_2 + O^+$	~1(-10)	18A-58	Cf. Table 18A-3, Reoctian 31.
34. $CO_2^+ + O_2 \rightarrow CO_2 + O_2^+$	5.0(-11)	18A-58	
35. $CO_2^+ + NO \rightarrow CO_2 + NO^+$	1.2(-10)	18A-58	
36. $CO_2^+ + H \rightarrow H^+ + CO_2$	~1(-10)	18A-63	Cf. Table 18A-3, Reaction 32.
37. $S^+ + NO \rightarrow NO^+ + S$	4.2(-10)	18A-64	
38. $SO_2^+ + O_2 \rightarrow O_2^+ + SO_2$	2.8(-10)	18A-64	

Table 18A-2. Negative-ion charge-transfer.

Reaction	$\overset{k}{(cm^3/sec)}$	References	Comments
1. $O^- + O_3 \rightarrow O + O_3^-$	5.3(-10)	18A-32	
2. $O^- + NO_2 \rightarrow O + NO_2^-$	1.2(-9)	18A-32	
3.* $O_2^- + O_3 \rightarrow O_2 + O_3^-$	4.0(-10)	18A-32	
4.* $O_2^- + NO_2 \rightarrow O_2 + NO_2^-$	8.0(-10)	18A-32	
5. $O_2^- + SO_2 \rightarrow SO_2^- + O_2$	4.8(-10)	18A-65	
6. $O_3^- + NO_2 \rightarrow$ Products	2.8(-10)	18A-41	
7. $NO^- + O_2 \rightarrow O_2^- + NO$	5.0(-10)	18A-66	
8. $H^- + NO_2 \rightarrow H + NO_2^-$	2.9(-9)	18A-32	
9. $OH^- + NO_2 \rightarrow OH + NO_2^-$	1.0(-9)	18A-32	
10. $O_2^- \cdot H_2O + O_3 \rightarrow$ Products	3(-10)	18A-65	
11. $O_2^-(H_2O)_2 + O_3 \rightarrow$ Products	3.4(-10)	18A-65	

*k for these reactions is little affected by one or two waters of hydration on the O_2^- ion (Reference 18A-65).

Table 18A-2. (Cont'd.)

Reaction	k (cm^3/sec)	References	Comments
12. $CO_4^- + O_3 \rightarrow O_3^- + CO_2 + O_2$	1.3(-10)	18A-65	
13. $SO_4^- + NO_2 \rightarrow NO_2^- + O_2 + SO_2$	2.5(-10)	18A-65	Also gives NO_3^-.

Table 18A-3. Positive-ion atom-interchange.

Reaction	k (cm^3/sec)	References	Comments
1.* $O^+ + N_2 \rightarrow N + NO^+$	1.2(-12)	18A-31, 33 47	See par. 18A.3.3.
2. $O^+ + N_2O \rightarrow NO^+ + NO$	2.3(-10)	18A-54	Cf. Table 18A-1, Reaction 8.
3. $O^+ + H_2 \rightarrow H + OH^+$	2.0(-9)	18A-62	
4. $O^+ + CO_2 \rightarrow CO + O_2^+$	1.1(-9)	18A-25, 31 47	Cf. Ref. 18A-25 for energy dependence.
5.* $N^+ + O_2 \rightarrow O + NO^+$	5.5(-10)	18A-4, 25, 33	Cf. Table 18A-1, Reaction 10.
6. $N^+ + H_2 \rightarrow H + NH^+$	5.6(-10)	18A-62	
7. $O_2^+ + N \rightarrow O + NO^+$	1.8(-10)	18A-31, 47	

* Recent data on the energy dependences of these reactions are collected in Reference 18A-33.

Table 18A-3. (Cont'd.)

Reaction	k (cm^3/sec)	References	Comments
8. $O_2^+ + N_2 \rightarrow NO + NO^+$	< 1.0(-15)	18A-31, 47	Not observed; rate constant limitation shown here is applicable at 300 and 600K.
9. $O_2^+ + H_2 \rightarrow$ Products	< 1.0(-11)	18A-62	
10. $O_2^+ + Na \rightarrow O + NaO^+$	7.7(-11)	18A-67	Cf. Table 18A-1, Reaction 17.
11. $N_2^+ + O \rightarrow N + NO^+$	1.4(-10)	18A-58, 60	*
12. $N_2^+ + H_2 \rightarrow H + N_2H^+$	1.7(-9)	18A-62	
13. $N_3^+ + O_2 \rightarrow$ Products	1.0±0.3(-10)	18A-46	200K
14. $O_4^+ + O \rightarrow O_2^+ + O_3$	~3(-10)	18A-68	
15. $O_4^+ + H_2O \rightarrow O_2 + O_2^+ \cdot H_2O$	1.5(-9)	18A-13	See par. 18A.3.11.
16. $N_4^+ + O_2 \rightarrow O_2^+ + N_2 + N_2$	4±1(-10)	18A-46	200K
17. $NO^+ + O_3 \rightarrow NO_2^+ + O_2$	< 1(-14)	18A-59	

*Energy dependence is given in Reference 18A-60. Branching ratio favors this over Reaction 18 of Table 18A-1 by 0.93/0.07.

Table 18A-3. (Cont'd.)

Reaction	k (cm^3/sec)	References	Comments
18. $H^{\cdot} + CO_2 \rightarrow HCO^{\cdot} \cdot O$	3(-9)	18A-63	
19. $S^{\cdot} \cdot C_2 \rightarrow SO^{\cdot} \cdot O$	1.6(-11)	18A-64	
20. $O_2^+ \cdot N_2 + O_2 \rightarrow N_2 + O_4^+$	1±0.5(-9)	Author's est.	
21. $O_2^+ \cdot N_2 + H_2O \rightarrow O_2^+ \cdot H_2O + N_2$	4±2(-9)	18A-13	
22.a. $O_2^+ \cdot H_2O + H_2O \rightarrow O_2 + OH + H_3O^+$	2(-10)	18A-13	See par. 18A.3.11.
b. $\rightarrow O_2 + H_3O^+ \cdot OH$	1.0(-9)	18A-13	
23. $NO^+ \cdot NO + H_2O \rightarrow NO^+ \cdot H_2O + NO$	1.4(-9)	18A-44	
24. $NO^+ \cdot H_2O + NO \rightarrow NO^+ \cdot NO + H_2O$	9(-14)	18A-44	296K
25. $NO^+ \cdot H_2O + H \rightarrow H_3O^+ + NO$	<7(-12)	18A-69	
26. $NO^+ \cdot H_2O + OH \rightarrow H_3O^+ + NO_2$	<6(-11)	18A-69	
27. $NO^+(H_2O)_3 + H_2O \rightarrow H_3O^+(H_2O)_2 + HNO_2$	7(-11)	18A-12, 43, 44	See por. 18A.3.12

Toble 18A-3. (Cont'd.)

Reactian	k (cm^3/sec)	References	Comments
28. $NO^+ \cdot CO_2 + H_2O \rightarrow NO^+ \cdot H_2O + CO_2$	~1(-9)	18A-46	See par. 18A.3.14.
29. $H_2O^+ + H_2O \rightarrow H_3O^+ + OH$	1.8(-9)	18A-21, 31	
30. $H_3O^+ \cdot OH + H_2O \rightarrow H_3O^+ \cdot H_2O + OH$	1.4(-9)	18A-13	
31. $CO_2^+ + O \rightarrow CO + O_2^+$	~1.6(-10)	18A-58	Cf. Toble 18A-1, Reoction 33.
32. $CO_2^+ + H \rightarrow HCO^+ + O$	6(-10)	18A-63	Cf. Table 18A-1, Reoction 36.
33. $No^+ + O_3 \rightarrow O_2 + NoO^+$	<1.0(-11)	18A-6	Not observed.
34. $K^+ + O_3 \rightarrow O_2 + KO^+$	<1.0(-11)	18A-6	Not observed.
35. $Mg^+ + O_3 \rightarrow O_2 + MgO^+$	2.3(-10)	18A-6	
36. $Co^+ + O_3 \rightarrow O_2 + CoO^+$	1.6(-10)	18A-6	
37. $Fe^+ + O_3 \rightarrow O_2 + FeO^+$	1.5(-10)	18A-6	
38. $U^+ + O_2 \rightarrow UO^+ + O$	8.5^{+4}_{-1}(-10)	18A-70	

Table 18A-3. (Cont'd.)

Reaction	k (cm^3/sec)	References	Comments
39. $U^+ + N_2 \rightarrow UN^+ + N$	<1(-11)	18A-70	
40. $MgO^+ + O \rightarrow O_2 + Mg^+$	~ 1.0(-11)	18A-6	
41. $SiO^+ + O \rightarrow O_2 + Si^+$	~ 2.0(-10)	18A-36	See par. 18A.3.5.

Table 18A-4. Negative-ion atom-interchange.

Reaction	k (cm^3/sec)	References	Comments
1. $O^- + N_2O \rightarrow NO + NO^-$	2.3±0.5(-10)	18A-71	
2. $O_3^- + N_2 \rightarrow O_2 + N_2O^-$	<1.0(-15)	18A-32	Not observed.
3. $O_3^- + NO \rightarrow O_2 + NO_2^-$	1.0(-11)	18A-32	Product identification (NO_3^- + O) given in Ref. 18A-32 is probably incorrect
4. $O_3^- + H \rightarrow OH^- + O_2$	8.4(-10)	18A-72	
5. $O_3^- + CO_2 \rightarrow O_2 + CO_3^-$	4.0(-10)	18A-32	*

* k for this reaction is slightly decreased for one water of hydration and drastically decreased for two (Reference 18A-65).

Table 18A-4. (Cont'd.)

Reaction	k (cm^3 sec)	References	Comments
6. $O_4^- \cdot O \rightarrow O_2 \cdot O_3^-$	4.0(-10)	18A-38	$2O_2 \cdot O^-$ may be a minor product channel.
7. $O_4^- \cdot NO \rightarrow O_2 \cdot NO_3^-$	2.5(-10)	18A-38	
8. $O_4^- \cdot H_2O \rightarrow O_2^- \cdot H_2O \cdot O_2$	1.4(-9)	18A-73	
9. $O_4^- \cdot CO_2 \rightarrow O_2 \cdot CO_4^-$	4.3(-10)	18A-38	
10. $NO_2^- \cdot O \rightarrow$ Products	<1.0(-11)	18A-74	Not observed.
11. $NO_2^- \cdot N \rightarrow$ Products	<1.0(-11)	18A-74	Not observed.
12.a. $NO_2^- \cdot H \rightarrow OH^- \cdot NO$ b. $\rightarrow HNO_2 \cdot e$	4(-10)	18A-72	$k_{12a} \geq 0.5\ k_{12}$; $0 \leq k_{12b} \leq k_{12}$
13. $NO_2^- \cdot O_3 \rightarrow O_2 \cdot NO_3^-$	1.8(-11)	18A-32	
14. $NO_2^- \cdot NO_2 \rightarrow NO \cdot NO_3^-$	~4.0(-12)	18A-38	See par. 18A.3.10.
15. $NO_3^- \cdot O \rightarrow$ Products	<1.0(-11)	18A-38	Not observed.

Table 18A-4. (Cont'd.)

Reaction	k (cm^3/sec)	References	Comments
16. $NO_3^- + N \rightarrow$ Products	$<1.0(-11)$	18A-38	Not observed.
17. $NO_3^- + NO \rightarrow NO_2 + NO_2^-$	$<1.0(-12)$	18A-38	See par. 18A.3.10.
18. $OONO^- + NO \rightarrow NO_2 + NO_2^-$	$\sim 1.5(-11)$	18A-40	
19. $CO_3^- + O \rightarrow CO_2 + O_2^-$	8.0(-11)	18A-32	
20. $CO_3^- + NO \rightarrow CO_2 + NO_2^-$	9.0(-12)	18A-32	*
21. $CO_3^- + NO_2 \rightarrow CO_2 + NO_3^-$	2(-10)	18A-72	*
22. $CO_4^- + O \rightarrow O_2 + CO_3^-$	1.5(-10)	18A-38	$CO_2 + O_3^-$ may be a minor product channel.
23. $CO_4^- + NO \rightarrow CO_2 + NO_3^-$	4.8(-11)	18A-38	
24. $O_2^- \cdot H_2O + NO \rightarrow H_2O + NO_3^-$	3.1(-10)	18A-40	
25. $O_2^- \cdot H_2O + CO_2 \rightarrow H_2O + CO_4^-$	5.8(-10)	18A-40	
26. $O_3^- \cdot H_2O + CO_2 \rightarrow$ Products	3(-10)	18A-65	

* k for these reactions is little affected by one water of hydration (Reference 18A-65).

Table 18A-4. (Cont'd.)

Reaction	k (cm^3 sec)	References	Comments
27. $O_3^-(H_2O)_2 + CO_2 \rightarrow$ Products	2(-10)	18A-65	
28. $NO_2^- \cdot H_2O + SO_2 \rightarrow NO_2^- \cdot SO_2 + H_2O$	1.5(-9)	18A-65	
29. $CO_3^- \cdot H_2O + NO \rightarrow$ Products	1.8(-11)	18A-65	
30. $CO_3^- \cdot H_2O + NO_2 \rightarrow$ Products	1.5(-10)	18A-65	

Table 18A-5. Three-body positive-ion reactions.

Reaction	k (cm^6/sec)	References	Comments
1. $O^+ + N_2 + He \rightarrow NO^+ + N + He$	5.4(-29)	18A-8	82K; N_2O^+ appears to form at first and then predissociate.
2. $O_2^+ + 2O_2 \rightarrow O_4^+ + O_2$	2.8(-30)	18A-20	307K; see par. 18A.3.8.
3. $O_2^+ + N_2 + N_2 \rightarrow O_2^+ \cdot N_2 + N_2$	8±4(-31)	18A-13	200K
4. $O_2^+ + N_2O + He \rightarrow O_2^+ \cdot N_2O + He$	5.2(-29)	18A-40	200K
5. $O_2^+ + H_2O + O_2 \rightarrow O_2^+ \cdot H_2O + O_2$	2.3(-28)	18A-13	296K; see par. 18A.3.11.
6. $O_2^+ + CO_2 + He \rightarrow O_2^+ \cdot CO_2 + He$	2.3(-29)	18A-40	200 K
7. $N_2^+ + N_2 + He \rightarrow N_4^+ + He$	1.2(-28) 1.9(-29)	18A-8 18A-8	82K 280K
8. $N_2^+ + 2N_2 \rightarrow N_4^+ + N_2$	5.0(-29)	18A-29	300K
9. $NO^+ + O_2 + He \rightarrow NO^+ \cdot O_2 + He$	<6(-34)	18A-46	200K
10. $NO^+ + N_2 + He \rightarrow NO^+ \cdot N_2 + He$	4(-30)	18A-74	90K *

* Because of the serious breakup problem, the equilibrium constant is more relevant than the rate constant alone; K is reported as <1(-19) at 200 and 225K (References 18A-46, 18A-75) and as >1(-20) at 298K (Reference 18A-76).

Table 18A-5. (Cont'd.)

Reaction	k (cm^6/sec)	References	Comments
11. $NO^+ + N_2 + NO \rightarrow NO^+ \cdot N_2 + NO$	2(-31)	18A-77	300K *
12. $NO^+ + 2NO \rightleftarrows NO^+ \cdot NO + NO$	5.0(-30)	18A-1	300K; reverse rate constant = 9(-16) cm^3/sec.
13. $NO^+ + H_2O + N_2 \rightarrow NO^+ \cdot H_2O + N_2$	1.5(-28)	18A-12, 43	300K; see par. 18A.3.12.
14. $NO^+ \cdot CO_2 + He \rightarrow NO^+ \cdot CO_2 + He$	1.0(-29)	18A-46	200K
15. $NO^+ + CO_2 + N_2 \rightarrow NO^+ \cdot CO_2 + N_2$	3(-29)	18A-46	200K
16. $NO^+ + CO_2 + CO_2 \rightarrow NO^+ \cdot CO_2 + CO_2$	2(-29)	18A-78	300K
17. $H_3O^+ + H_2O + O_2 \cdot H_3O^+ \cdot H_2O + O_2$	3.7(-27)	18A-21	307K } Reverse rate constant =7(-26) cm^3/sec.
18. $H_3O^+ + H_2O + N_2 \rightarrow H_3O^+ \cdot H_2O + N_2$	3.4(-27)	18A-21	300K }
19. $H_3O^+ \cdot H_2O + H_2O + O_2 \rightleftarrows H_3O^+(H_2O)_2 + O_2$	2.0(-27)	18A-21	307K } Reverse rate constant =7(-18) cm^3/sec.
20. $H_3O^+ \cdot H_2O + H_2O + N_2 \rightleftarrows H_3O^+(H_2O)_2 + N_2$	2.3(-27)	18A-21	300K }

* Because of the serious breakup problem, the equilibrium constant is more relevant than the rate constant alone; K is reported as < 1(-19) at 200 and 225K (References 18A-46, 18A-75) and as > 1(-20) at 298K (Reference 18A-76).

Table 18A-5. (Cont'd.)

Reaction	k (cm^6/sec)	References	Comments
21. $H_3O^+(H_2O)_2 + H_2O + O_2 \rightleftharpoons H_3O^+(H_2O)_3 + O_2$	2.0(-27)	18A-21	307K } Reverse rate constant = 4.0(-14) cm^3/sec.
22. $H_3O^+(H_2O)_2 + H_2O + N_2 \rightleftharpoons H_3O^+(H_2O)_3 + N_2$	2.4(-27)	18A-21	300K }
23. $H_3O^+(H_2O)_3 + H_2O + O_2 \rightleftharpoons H_3O^+(H_2O)_4 + O_2$	9.0(-28)	18A-21	307K; reverse rate constant = 6.0(-12) cm^3/sec.
24. $NO^+ \cdot H_2O + H_2O + N_2 \rightarrow NO^+(H_2O)_2 + N_2$	1.1(-27)	18A-12, 43	300K; see par. 18A.3.12.
25. $NO^+(H_2O)_2 + H_2O + N_2 \rightarrow NO^+(H_2O)_3 + N_2$	1.6(-27)	18A-12, 43	300K; see par. 18A.3.12.
26. $Mg^+ + O_2 + Ar \rightarrow MgO_2^+ + Ar$	~2.5(-30)	18A-6	300K
27. $Ca^+ + O_2 + Ar \rightarrow CaO_2^+ + Ar$	~6.6(-30)	18A-6	300K
28. $Fe^+ + O_2 + Ar \rightarrow FeO_2^+ + Ar$	~1.0(-30)	18A-6	300K
29. $K^+ + CO_2 + CO_2 \rightleftharpoons K^+ \cdot CO_2 + CO_2$	4^{+4}_{-2}(-30)	18A-79	Reverse rate constant = $2.5^{+2.5}_{-1.3}$(-13) cm^3/sec.
30. $Na^+ + CO_2 + CO_2 \rightleftharpoons Na^+ \cdot CO_2 + CO_2$	2(-29±0.5)	18A-80	Reverse rate constant = 1(-14±0.5) cm^3/sec.
31. $Na^+ \cdot CO_2 + CO_2 + CO_2 \rightleftharpoons Na^+(CO_2)_2 + CO_2$	2(-29±0.5)	18A-80	Reverse rate constant = 5(-13±0.5) cm^3/sec.

Table 18A-6. Three-body negative-ion reactions.

Reaction	k (cm^6 sec)	References	Comments
1. $O^- + 2O_2 \rightarrow O_3^- + O_2$	1.2(-30) 1.05(-30)	18A-73 18A-81	300K 298K
2. $O^- + N_2 + He \rightarrow N_2O^- \cdot He$	1.3(-30) ~4.0(-31)	18A-32 18A-40	80K 200K
3. $O^- + H_2O + O_2 \rightarrow O^- \cdot H_2O + O$	1.0(-28)	18A-73	300K
4. $O^- + CO_2 + CO_2 \rightarrow CO_3^- \cdot CO_2$	8.0(-29)	18A-82	300K
5. $C_2^- + C_2 + O_2 \rightleftharpoons O_4^- + O_2$	3.0(-31) 4.0(-31) 3.0(-31)	18A-39 18A-73 18A-81	310K; see par. 18A.3.9. 300K; reverse rate constant = 2.7(-14) cm^3/sec. 298K
6. $O_2^- + N_2 + He \rightarrow C_2^- \cdot N_2 + He$	~4.0(-32)	18A-40	200K
7. $O_2^- + H_2O + O_2 \rightarrow O_2^- \cdot H_2O + O_2$	3(-28)	18A-73	300K
8. $O_2^- + CO_2 + O_2 \rightarrow CO_4^- + O_2$	4.7(-29)	18A-65	300K
9. $O_2^- + CO_2 + CO_2 \rightarrow CO_4^- \cdot CO_2$	9.0(-30)	18A-82	300K
10. $O_3^- + H_2O + O_2 \rightarrow O_3^- \cdot H_2O + O_2$	2.1(-28)	18A-73	300K

Table 18A-6. (Cont'd.)

Reaction	k (cm^6/sec)	References	Comments
11. $NO_2^- \cdot H_2O + NO \rightarrow NO_2^- \cdot H_2O + NO$	1.3(-28)	18A-1	300K
12. $O_2^- \cdot H_2O + H_2O + O_2 \rightarrow O_2^-(H_2O)_2 + O_2$	4(-28)	18A-73	300K

Table 18A-7. Charge transfer to neutral metals.*

Reaction	Measured cross-section for ions of 1 eV (at the center of mass) (cm^2)	Extrapolated value of thermal-energy rate constant (cm^3/sec)**
$N^+ + Na \rightarrow N + Na^+$	small	
$O^+ + Na \rightarrow O + Na^+$	small	
$N_2^+ + Na \rightarrow N_2 + Na^+$	3.0×10^{-15}	1.9×10^{-9}
$O_2^+ + Na \rightarrow O_2 + Na^+$	5.5×10^{-15}	1.4×10^{-9}
$NO^+ + Na \rightarrow NO + Na^+$	1.2×10^{-15}	
$H_2O^+ + Na \rightarrow H_2O + Na^+$	2.8×10^{-14}	2.7×10^{-9}
$H_3O^+ + Na \rightarrow H_3O + Na^+$	2.4×10^{-14}	
$N_2O^+ + Na \rightarrow N_2O + Na^+$	2.7×10^{-14}	2.0×10^{-9}
$Na^+ + Na \rightarrow Na + Na^+$	2.3×10^{-14}	2.8×10^{-9}
$N^+ + Mg \rightarrow N + Mg^+$	1.1×10^{-14}	1.2×10^{-9}
$O^+ + Mg \rightarrow O + Mg^+$	small	
$N_2^+ + Mg \rightarrow N_2 + Mg^+$	1.8×10^{-14}	
$O_2^+ + Mg \rightarrow O_2 + Mg^+$	7.6×10^{-15}	1.2×10^{-9}
$NO^+ + Mg \rightarrow NO + Mg^+$	1.4×10^{-14}	1.0×10^{-9}
$H_2O^+ + Mg \rightarrow H_2O + Mg^+$	1.8×10^{-14}	2.2×10^{-9}
$H_3O^+ + Mg \rightarrow H_3O + Mg^+$	8.8×10^{-15}	
$N_2O^+ + Mg \rightarrow N_2O + Mg^+$	2.6×10^{-14}	2.1×10^{-9}
$Mg^+ + Mg \rightarrow Mg + Mg^+$	3.8×10^{-14}	4.7×10^{-9}
$N^+ + Ca \rightarrow N + Ca^+$	5.3×10^{-15}	1.1×10^{-9}

Table 18A-7. (Cont'd)

Reaction	Measured cross-section for ions of 1 eV (at the center of mass) (cm^2)	Extrapolated value of thermal-energy rate constant (cm^3/sec)**
$O^+ + Ca \rightarrow O + Ca^+$	1.1×10^{-14}	7.5×10^{-10}
$N_2^+ + Ca \rightarrow N_2 + Ca^+$	3.0×10^{-14}	1.7×10^{-9}
$O_2^+ + Ca \rightarrow O_2 + Ca^+$	1.5×10^{-14}	4.1×10^{-9}
$NO^+ + Ca \rightarrow NO + Ca^+$	2.2×10^{-14}	4.0×10^{-9}
$H_2O^+ + Ca \rightarrow H_2O + Ca^+$	5.5×10^{-14}	4.0×10^{-9}
$H_3O^+ + Ca \rightarrow H_3O + Ca^+$	3.4×10^{-14}	4.4×10^{-9}
$N_2O^+ + Ca \rightarrow N_2O + Ca^+$	4.5×10^{-14}	3.7×10^{-9}
$Ca^+ + Ca \rightarrow Ca + Ca^+$	6.0×10^{-14}	
	Measured cross-section for ions of 3 eV (at the center of mass) (cm^2)	
$H^+ + Fe \rightarrow H + Fe^+$	9.5×10^{-16}	
$N^+ + Fe \rightarrow N + Fe^+$	1.6×10^{-16}	1.5×10^{-9}
$O^+ + Fe \rightarrow O + Fe^+$	1.3×10^{-15}	2.9×10^{-9}
$N_2^+ + Fe \rightarrow N_2 + Fe^+$	2.9×10^{-15}	4.3×10^{-10}
$NO^+ + Fe \rightarrow NO + Fe^+$	2.4×10^{-15}	9.1×10^{-10}
$O_2^+ + Fe \rightarrow O_2 + Fe^+$	2.0×10^{-15}	1.2×10^{-9}
$H_2O^+ + Fe \rightarrow H_2O + Fe^+$	3.3×10^{-15}	1.5×10^{-9}

* Table kindly supplied by J.A. Rutherford (Reference 18A-83). Cf. also References 18A-84 through 18A-88.

** Extrapolation scheme described in Reference 18A-89.

REFERENCES

18A-1. Lineberger, W.C., and L.J. Puckett, Phys. Rev. 186, 116 (1969); Ibid. 187, 286 (1969); Ibid. A1, 1635 (1970).

18A-2. Copsey, M.J., D. Smith, and J. Sayers, Planet. Space Sci. 14, 1047 (1966).

18A-3. Smith, D., and R.A. Fouracre, Planet. Space Sci. 16, 243 (1968).

18A-4. Dunkin, D.B., F.C. Fehsenfeld, A.L. Schmeltekopf, and E.E. Ferguson, J. Chem. Phys. 49, 1365 (1968).

18A-5. Ferguson, E.E., D.K. Bohme, F.C. Fehsenfeld, and D.B. Dunkin, J. Chem. Phys. 50, 5039 (1969).

18A-6. Ferguson, E.E., and F.C. Fehsenfeld, J. Geophys. Res. 73, 6215 (1968).

18A-7. Bohme, D.K., D.B. Dunkin, F.C. Fehsenfeld, and E.E. Ferguson, J. Chem. Phys. 49, 5201 (1968).

18A-8. Bohme, D.K., D.B. Dunkin, F.C. Fehsenfeld, and E.E. Ferguson, J. Chem. Phys. 51, 863 (1969).

18A-9. Fehsenfeld, F.C., M. Mosesman, and E.E. Ferguson, J. Chem. Phys. 55, 2115 (1971).

18A-10. Farragher, A.L., J.A. Peden, and W.L. Fite, J. Chem. Phys. 50, 287 (1969).

18A-11. Howard, C.J., H.W. Rundle, and F. Kaufman, J. Chem. Phys. 53, 3745 (1970).

18A-12. Howard, C.J., H.W. Rundle, and F. Kaufman, J. Chem. Phys. 55, 4772 (1971).

18A-13. Howard, C.J., V.M. Bierbaum, H.W. Rundle, and F. Kaufman, J. Chem. Phys. 57, 3491 (1972).

18A-14. Fehsenfeld, F.C., D.L. Albritton, J.A. Burt, and H.I. Schiff, Can. J. Chem. 47, 1793 (1969).

18A-15. Albritton, D.L., A.L. Schmeltekopf, and E.E. Ferguson, Bull. Am. Phys. Soc. 13, 212 (1968).

18A-16. Warneck, P., J. Chem. Phys. 47, 4279 (1967).

18A-17. Warneck, P., Planet. Space Sci. 15, 1349 (1967).

18A-18. Paulson, J.F., R.L. Mosher, and F. Dale, J. Chem. Phys. 44, 3025 (1966).

18A-19. Paulson, J.F., Adv. Chem. 58, 28 (1966).

18A-20. Durden, D.A., P. Kebarle, and A. Good, J. Chem. Phys. 50, 805 (1969).

18A-21. Good, A., D.A. Durden, and P. Kebarle, J. Chem. Phys. 52, 212, 222 (1970).

18A-22. Turner, B.R., and J.A. Rutherford, J. Geophys. Res. 73, 6751 (1968).

18A-23. Turner, B.R., J.A. Rutherford, and D.M.J. Compton, J. Chem. Phys. 48, 1602 (1968).

18A-24. Heimerl, J., R. Johnsen, and M.A. Biondi, J. Chem. Phys. 51, 5041 (1969).

18A-25. Johnsen, R., H.L. Brown, and M.A. Biondi, J. Chem. Phys. 52, [illegible] (1970).

18A-26. Golden, D.E., G. Sinnott, and R.N. Varney, Phys. Rev. Letts. 20, 23[illegible] (196[illegible]).

18A-27. Bohme, D.K., P.P. Ong, J.B. Hasted, and L.R. Megill, Planet. Space Sci. 1[illegible], 1777 (19[illegible]).

18A-28. Ong, P.P., and J.B. Hasted, [illegible] Phys. [illegible], [illegible] (19[illegible]).

18A-29. Miller, T.M., J.T. Moseley, D.W. Martin, and E.W. McDaniel, Phys. Rev. Letts. 21, [illegible] (1968).

18A-30. [illegible], Y., [illegible], and [illegible], Mass Spectrosc. 1[illegible], [illegible] (19[illegible]).

18A-31. [illegible], Can. J. Chem. 47, 17[illegible] (19[illegible]).

18A-32. Ferguson, E.E., Can. J. Chem. 47, [illegible] (19[illegible]).

18A-33. McFarland, M., D.L. Albritton, F.C. Fehsenfeld, E.E. Ferguson, and A.L. Schmeltekopf, J. Chem. Phys. [illegible], [illegible] (197[illegible]).

18A-34. Schmeltekopf, A.L., E.E. Ferguson, and F.C. Fehsenfeld, J. Chem. Phys. 4[illegible], 2[illegible] (196[illegible]).

18A-35. O'Malley, T.F., J. Chem. Phys. [illegible], [illegible] (1970).

18A-36. Fehsenfeld, F.C., Can. J. Chem. 47, 1[illegible] (19[illegible]).

18A-37. Fehsenfeld, F.C., and E.E. Ferguson, J. Geophys. Res. 73, 2217 (1968).

18A-38. Fehsenfeld, F.C., E.E. Ferguson, and D.K. Bohme, Planet. Space Sci. 17, 17[illegible] (19[illegible]).

18A-39. McKnight, L.G., and J.M. Sawina, DASA Symposium on Physics and Chemistry of the Upper Atmosphere, Stanford Research Institute (1969).

18A-40. Adams, N.G., D.K. Bohme, D.B. Dunkin, F.C. Fehsenfeld, and E.E. Ferguson, J. Chem. Phys. 52, 3133 (1970).

18A-41. Dunkin, D.B., F.C. Fehsenfeld, and E.E. Ferguson, Chem. Phys. Letts. 15, 257 (1972).

18A-42. Ferguson, E.E., D.B. Dunkin, and F.C. Fehsenfeld, J. Chem. Phys. 57, 1459 (1972).

18A-43. Fehsenfeld, F.C., M. Mosesman, and E.E. Ferguson, J. Chem. Phys. 55, 2120 (1971).

18A-44. Puckett, L.J., and M.W. Teague, J. Chem. Phys. 54, 2564 (1971).

18A-45. Fehsenfeld, F.C., E.E. Ferguson, and M. Mosesman, Chem. Phys. Letts. 4, 73 (1969).

18A-46. Dunkin, D.B., F.C. Fehsenfeld, A.L. Schmeltekopf, and E.E. Ferguson, J. Chem. Phys. 54, 3817 (1971).

18A-47. Ferguson, E.E., Revs. Geophys. 5, 305 (1967).

18A-48. Lindinger, W., F.C. Fehsenfeld, A.L. Schmeltekopf, and E.E. Ferguson, J. Geophys. Res. 79, 4753 (1974).

18A-49. Bohme, D.K., N.G. Adams, M. Mosesman, D.B. Dunkin, and E.E. Ferguson, J. Chem. Phys. 52, 5094 (1970).

18A-50. Stebbings, R.F., and J.A. Rutherford, J. Geophys. Res. 73, 1035 (1968).

18A-51. Fehsenfeld, F.C., and E.E. Ferguson, J. Chem. Phys. 56, 3066 (1972).

18A-52. McFarland, M., D.L. Albritton, F.C. Fehsenfeld, A.L. Schmeltekopf, and E.E. Ferguson, J. Geophys. Res. 79, 2005 (1974).

18A-53. Dunkin, D.B., M. McFarland, F.C. Fehsenfeld, and E.E. Ferguson, J. Geophys. Res. 76, 3820 (1971).

18A-54. Ryan, E.R., J. Chem. Phys. 57, 271 (1971).

18A-55. Ferguson, E.E., F.C. Fehsenfeld, P.D. Goldan, and A.L. Schmeltekopf, J. Geophys. Res. 70, 4323 (1965).

18A-56. Lindinger, W., M. McFarland, F.C. Fehsenfeld, A.L. Schmeltekopf, and E.E. Ferguson, J. Chem. Phys. in press (1975).

18A-57. Lindinger, W., D.L. Albritton, F.C. Fehsenfeld, and E.E. Ferguson, J. Geophys. Res., in press (1975).

18A-58. Fehsenfeld, F.C., D.B. Dunkin, and E.E. Ferguson, Planet. Space Sci. 18, 1267 (1970).

18A-59. Fehsenfeld, F.C., E.E. Ferguson, and C.J. Howard, J. Geophys. Res. 78, 327 (1973).

18A-60. McFarland, M., D.L. Albritton, F.C. Fehsenfeld, E.E. Ferguson, and A.L. Schmeltekopf, J. Geophys. Res. 79, 2925 (1974).

18A-61. Ferguson, E.E., F.C. Fehsenfeld, P.D. Goldan, A.L. Schmeltekopf, and H.I. Schiff, Planet. Space Sci. 13, 823 (1965).

18A-62. Fehsenfeld, F.C., A.L. Schmeltekopf, and E.E. Ferguson, J. Chem. Phys. 46, 2802 (1967).

18A-63. Fehsenfeld, F.C., and E.E. Ferguson, J. Geophys. Res. 76, 8453 (1971).

18A-64. Fehsenfeld, F.C., and E.E. Ferguson, J. Geophys. Res. 78, 1699 (1973).

18A-65. Fehsenfeld, F.C., and E.E. Ferguson, J. Chem. Phys. 61, 3181 (1974).

18A-66. McFarland, M., D.B. Dunkin, F.C. Fehsenfeld, A.L. Schmeltekopf, and E.E. Ferguson, J. Chem. Phys. 56, 2358 (1972).

18A-67. Rol, P.E., and E.A. Entemann, J. Chem. Phys. 49, 1439 (1968).

18A-68. Fehsenfeld, F.C., and E.E. Ferguson, Radio Sci. 7, 113 (1972).

18A-69. Fehsenfeld, F.C., C.J. Howard, W. Harrop, and E.E. Ferguson, J. Geophys. Res., in press (1975).

18A-70. Johnsen, R., and M.A. Biondi, J. Chem. Phys. 57, 1975 (1972).

18A-71. Marx, R., G. Mauclaire, F.C. Fehsenfeld, D.B. Dunkin, and E.E. Ferguson, J. Chem. Phys. 58, 3267 (1973).

18A-72. Fehsenfeld, F.C., C.J. Howard, and E. E. Ferguson, J. Chem. Phys. 58, 5841 (1973).

18A-73. Pack, J.L., and A.V. Phelps, Bull. Am. Phys. Soc. 16, 214 (1971).

18A-74. Fehsenfeld, F.C., unpublished results.

18A-75. Biondi, M.A., DASIAC Reaction Rate Data, No. 44, p. 4 (1974).

18A-76. Heimerl, J.M., and J.A. Vanderhoff, J. Chem. Phys. 60, 4262 (1974).

18A-77. Heimerl, J.M., and J.A. Vanderhoff, American Geophysical Union Meeting, San Francisco, California (1971).

18A-78. Heimerl, J.M., and L.J. Puckett, Trans. Am. Geophys. Union 52, 303 (1971).

18A-79. Keller, G.E., and R.A. Beyer, Bull. Am. Phys. Soc. 16, 214 (1971).

18A-80. Keller, G.E., and R.A. Beyer, J. Geophys. Res. 76, 288 (1971).

18A-81 Parkes, D.A., Trans. Faraday Soc. 67, 711 (1971).

18A-82. Moruzzi, J.L., and A.V. Phelps, J. Chem. Phys. 45, 4617 (1966).

18A-83. Turner, B.R., and J.A. Rutherford, Gulf General Atomic, Report GA-9827 (1970).

18A-84. Rutherford, J.A., R.F. Mathis, B.R. Turner, and D.A. Vroom, J. Chem. Phys. 55, 3785 (1971).

18A-85. Rutherford, J.A., and D.A. Vroom, J. Chem. Phys. 55, 5022 (1971).

18A-86. Rutherford, J.A., R.F. Mathis, B.R. Turner, and D.A. Vroom, J. Chem. Phys. 56, 4654 (1972).

18A-87. Rutherford, J.A., R.F. Mathis, B.R. Turner, and D.A. Vroom, J. Chem. Phys. 57, 3087 (1972).

18A-88. Rutherford, J.A., and D.A. Vroom, J. Chem. Phys. 57, 3091 (1972).

18A-89. Wolf, F.A., and B.R. Turner, J. Chem. Phys. 48, 4226 (1968).

THIS PAGE IS INTENTIONALLY LEFT BLANK.

18. ION-NEUTRAL REACTIONS
B. NON-THERMAL PROCESSES

David A. Vroom, John A. Rutherford, and Richard L. Vaigt
IRT Corporation

(Latest Revision 9 October 1974)

DDC
RECEIVED
DEC 8 1975
D

18B.1 INTRODUCTION

The principal purpose of this chapter is to supply a compilation of data on ion-molecule and charge-transfer reactions which are of interest in atmospheric chemistry and physics. The constraint imposed by considering only reactions involving atmospheric species has led to the exclusion of a great deal of interesting information on other, non-atmospheric, ion-neutral processes.

The ion-energy range covered by the data in this chapter has been set arbitrarily at approximately 1-500 eV. The lower limit of this range was determined by the earlier lack of data for most reactions in the region between thermal energies and approximately one electron volt. Thermal energy data are presented in Chapter 18A. More recently, however, considerable data obtained by the use of flowing-afterglow drift-tube methods have become available, and these data do cover the energy regime from near-thermal to several electron volts. The latter information, together with results from drift-tube experiments, have been included wherever available. The upper limit of 500 eV was set arbitrarily such as to be greater than the energies of most experiments which measure in the low ion-energy region. Chapter 18C includes data at still higher energies.

18B.2 TECHNIQUES

The various techniques employed are for the most part described in Chapter 7. The exception is that of the flowing-afterglow drift tube, which has only recently been developed. A complete description of this method is given in Reference 18B-1.

The bulk or portion of ion-neutral data obtained in the energy range above one electron volt has come from experiments employing ion beams. The beam-gas technique, as employed by Giese and Maier (References 18B-2 through 18B-6), and the crossed-beam technique of Stebbings, Rutherford, and Turner (References

DISTRIBUTION STATEMENT A
Approved for public release;
Distribution Unlimited

Revision No. 5, June 1975

18B-5, 18B-6), are typical of experiments of this nature. Both of these employ double-mass-spectrometer systems; in each instance the first mass spectrometer is used to select the primary ion to be studied, and the second to analyze the products of collisions between the primary ions and neutral species. In order to obtain more information on the energetics of ion-neutral reactions, Paulson, Dale, and Studniarz (Reference 18B-7) have used the double-mass-spectrometer concept in conjunction with time-of-flight techniques. This incorporation of time-of-flight allows the translational energy of the product species to be measured.

Another beam technique, merging beams, has been described in two review articles (References 18B-8, 18B-9). This method has the advantage of facilitating the study of reactions in the energy range from near-thermal to several hundreds of electron volts; it can also give information on the kinetic energy of the products of reaction.

Still other methods which have been employed are the mass-spectrometer ion-source experiment (Reference 18B-10) and various drift-tube techniques (References 18B-11 through 18B-13). Both these and the flowing-afterglow drift-tube experiment (Reference 18B-11) give data in the energy range from near-thermal to several electron volts. The two drift techniques show promise of being extremely useful for obtaining cross-section data in the near-thermal-energy region.

18B.3 PRESENTATION OF DATA

Most of the data given here cover a considerable energy range and as a consequence are presented in the form of graphs. In order to simplify use of the graphical material, all the information pertaining to a given reaction is provided in the figure caption referring to that reaction. These figure captions include references to the workers who obtained the data, together with the technique(s) employed, any data available about the effects of excited states of the primary ions, any data available about the states of the product species, and other relevant information which may be helpful.

Rate coefficients for a number of reactions which have been measured at only one ion energy in the non-thermal region are presented in tabular form.

18B.3.1 Graphical Data

Two types of graph are included:

(A) The first type (in Subsections 18B.3.1.1 through 18B.3.1.15) is used for data obtained at higher energies (~1-500 eV). In these graphs, the ordinate gives the cross section for the reaction and the abscissa, the ion velocity related to that cross-section. This velocity is obtained directly from the ion energy. The use of velocity on the abscissa conforms with the format used in Chapter 15. It should be noted, however, that the ion velocity does not account for any motion of the neutral primary species. In most cases the neutral primary is at room temperature (300 K) and its motion is not of importance. For some atomic species which are formed by thermal dissociation the motion of the neutral can, however, become appreciable. The ion velocity will then be found to differ from the velocity in the center-of-mass system at low collision energies. The motion of both species is accounted for when the barycentric or collision energy is considered. This parameter is given across the top axis of each figure.

Data obtained using merging beams are plotted in the same format as is used for other beam data. Here, the collision energy is the energy at the center-of-mass of these experiments. The ion velocity given on the abscissa is obtained by taking a reasonable value for the neutral velocity and computing the corresponding ion velocity. The neutral velocity chosen is that which would be expected in a beam-gas or crossed-beam experiment involving the same species.

The higher ion-energy (~1-500 eV) data graphs are organized as follows:

1) Data for each neutral reactant are grouped together in a given subsection. These subsections are arranged in the following order: The atomic neutral species come first (Subsections 18B.3.1.1 through 18B.3.1.7) in order of increasing atomic weight followed by diatomic (Subsections 18B.3.1.8 through 18B.3.1.10) and then triatomic (Subsections 18B.3.1.11 through 18B.3.1.15) molecular species, each in order of increasing molecular weight.

2) Within each neutral reactant subsection, the data for positive-ion reactions precede those for negative-ion processes within this grouping the data for the atomic reactant ions precede those for molecular ions. The atomic and molecular ions are arranged in order of increasing atomic or molecular weight.

3) For a given set of reactants, if data on formation of more than one set of products are available, the following procedure is followed: If only one or two determinations of each cross-section are used, the data are combined on one plot. If considerable data are available for the different reaction channels, the data are given in different plots which are then ordered as follows:

a) Charge transfer;
b) Dissociative charge transfer;
c) Ion-molecule processes, in order of increasing weight of the product neutral species.

B) The second type of graph (in Subsection 18B.3.1.16) is used to present data obtained using drift tubes or flowing-afterglow drift tubes. In these figures the rate constant is plotted on the ordinate. For drift-tube data, the electric field strength per unit pressure (E/P) is used on the abscissa and the average ion energy is placed at the top of the figure. For the flowing-afterglow drift-tube studies the energy at the center-of-mass is given on the abscissa and values of electric field strength per unit number density (E/N) are given at the top of the figure. These formats conform with those commonly used by workers in the field.

The reactions are ordered in the same fashion as for the higher-energy data. That is, the information on atomic neutral species precedes that for molecular species and each group is arranged in order of increasing atomic or molecular weight.

18B.3.1.1 O-Atom Reactions

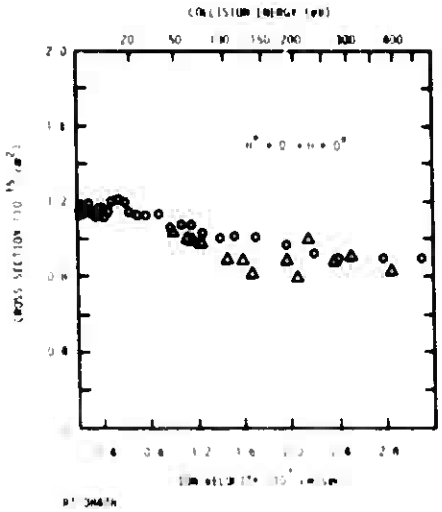

Figure 18B-1. Cross-section for the reaction $H^+ + O \rightarrow H + O^+$. Circles are the data of Rutherford and Vroom (Reference 18B-14) obtained using crossed-beam techniques and O atoms produced by thermal dissociation. Triangles are the data of Stebbings, Smith, and Ehrhardt (Reference 18B-15) obtained using crossed-beam techniques and O atoms produced in an RF discharge.

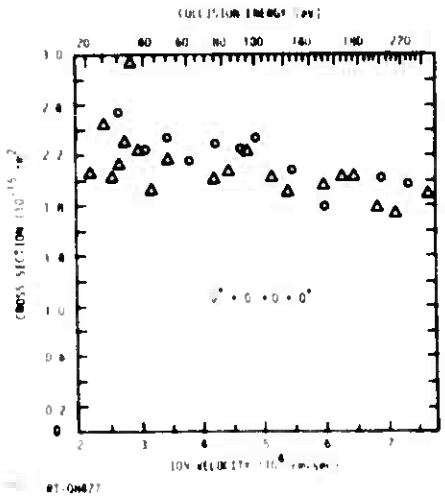

Figure 18B-2. Cross-section for the reaction $O^+ + O \rightarrow O + O^+$. Circles are the data of Rutherford and Vroom (Reference 18B-14) obtained using crossed-beam techniques and O atoms produced by thermal dissociation. Triangles are the data of Stebbings, Smith, and Ehrhardt (Reference 18B-15) obtained using crossed-beam techniques and O atoms produced in an RF discharge.

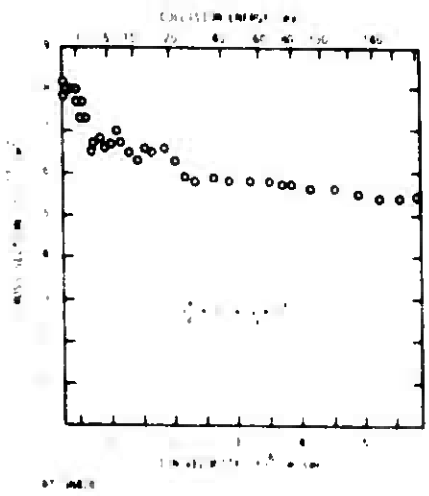

Figure 18B-3. Cross-section for the reaction $N_2^+ + O \rightarrow N_2 + O^+$. Circles are the data of Rutherford and Vroom (Reference 18B-14) obtained using crossed-beam techniques and O atoms produced by thermal dissociation.

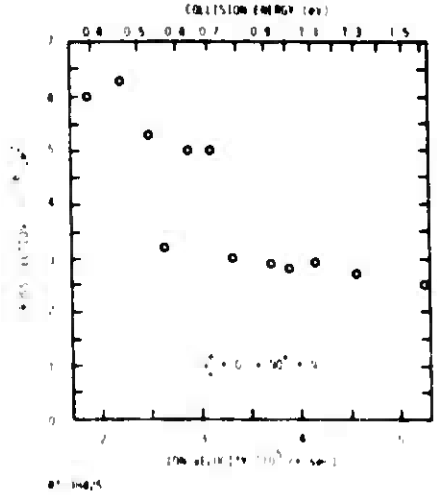

Figure 18B-4. Cross-section for the reaction $N_2^+ + O \rightarrow NO^+ + N$. Circles are the data of Rutherford and Vroom (Reference 18B-14) obtained using crossed-beam techniques and O atoms produced by thermal dissociation.

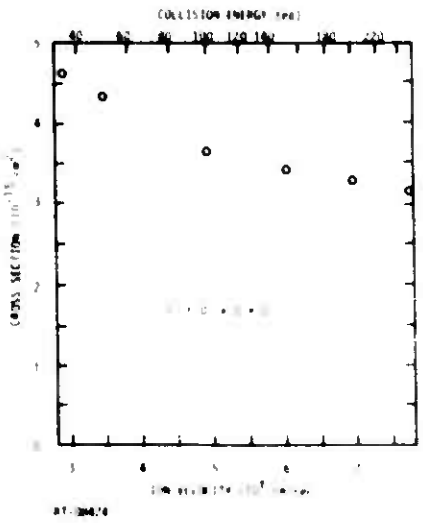

Figure 188-5. Cross section for the reaction $O^- + C \rightarrow O + O^-$. Circles are the data of Rutherford and Vroom (Reference 188-14) obtained using crossed beam techniques and O atoms produced by thermal dissociation

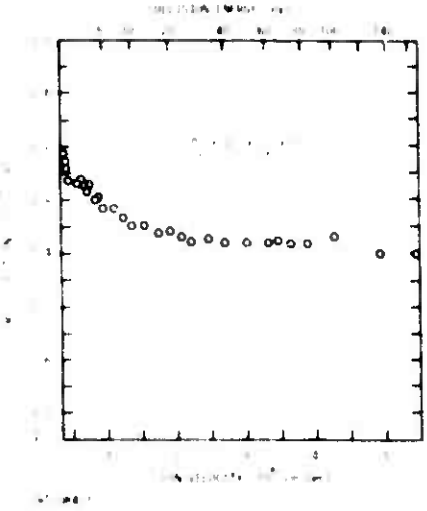

Figure 188-6. Cross section for the reaction $O_2^- + O \rightarrow O_2 + O^-$. Circles are the data of Rutherford and Vroom (Reference 188-14) obtained using crossed beam techniques and O atoms produced by thermal dissociation.

188.3.1.2 Na-Atom Reactions

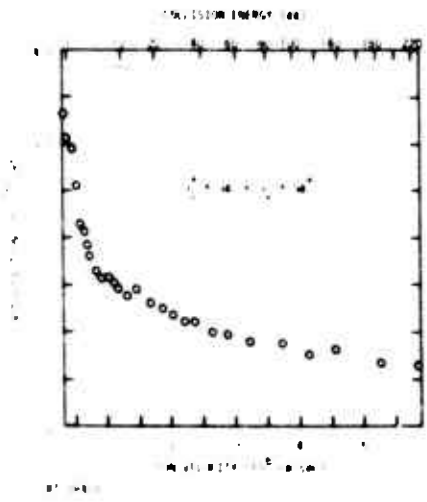

Figure 188-7. Cross section for the reaction $N_2^+ + Na \rightarrow N_2 + Na^+$. Circles are the data of Rutherford et al (Reference 188-16) obtained using crossed-beam techniques.

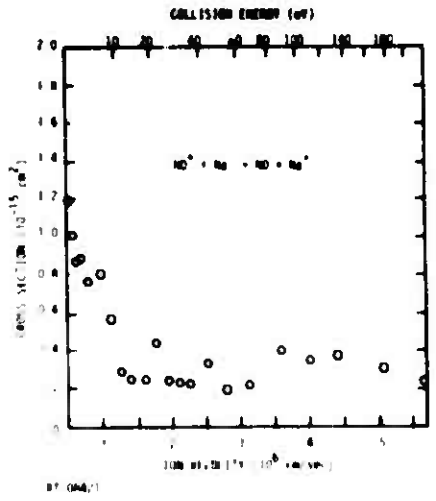

Figure 188-8. Cross section for the reaction $NO^+ + Na \rightarrow NO + Na^+$. Circles are the data of Rutherford et al (Reference 188-16) obtained using crossed-beam techniques.

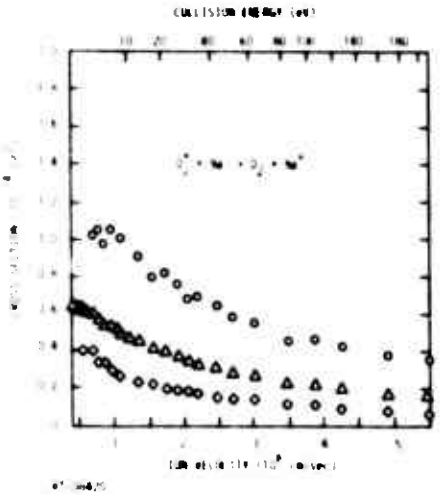

Figure 188-9 Cross-sections for the reaction $O_2^+ + Ne \rightarrow O_2 + Na^+$. Diamonds are the dete for ground-state O_2^+, circles are the data for metasteble O_2^+, end triengles ara the data for e composita beam of O_2^+ in which 32% of the O_2^+ is excited All dete are from Ruther ford et al (Reference 188 16) obteined using crossed beam techniques

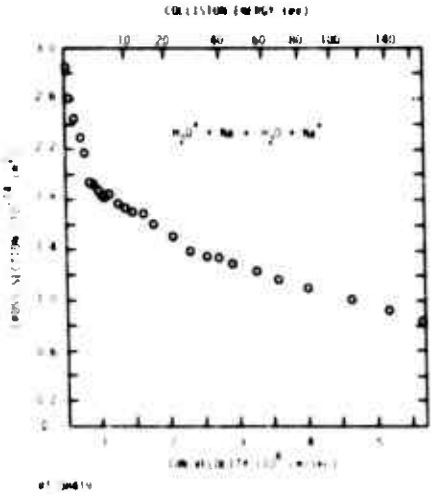

Figure 188-10. Cross-section for the reaction $H_2O^+ + Na \rightarrow H_2O + Na^+$. Circles are the data of Rutherford at al (Reference 188-16) obtained using crossed-beam techniques.

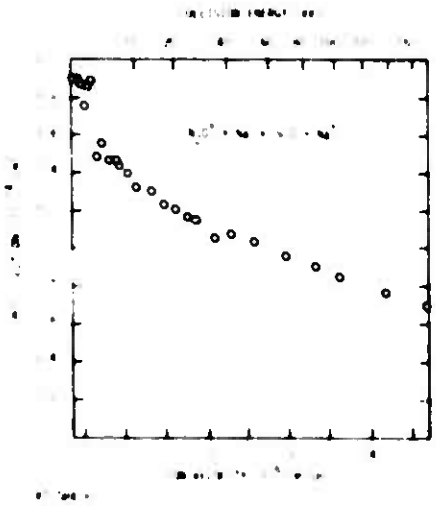

Figure 188 11 Cross section for the reaction $N_2O^+ + N_2 \rightarrow N_2O + Ne^+$ Circles ara the data of Rutherford et al (Reference 188 16) obteined using crossed beam techniques

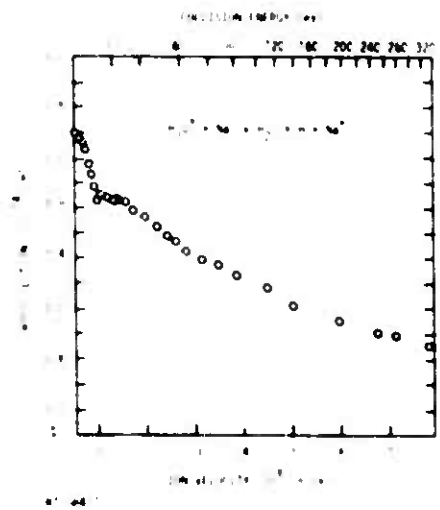

Figure 188 12 Cross section for the reaction $H_3O^+ + Ne \rightarrow H_2O + H + Na^+$ Circles ara the data of Rutherford et al (Raferance 188 t6) obtained using crossed-beam techniques

188.3.1.3 Mg-Atom Reactions

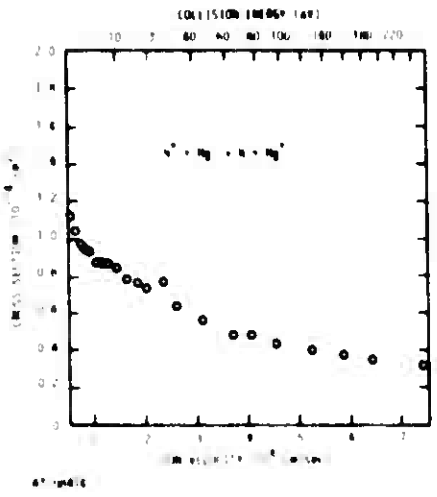

Figure 188-13. Cross-section for the reaction $N^+ + Mg \rightarrow N + Mg^+$. Circles are the date of Rutherford et el (Reference 188 6) obtained using crossed-beam techniques.

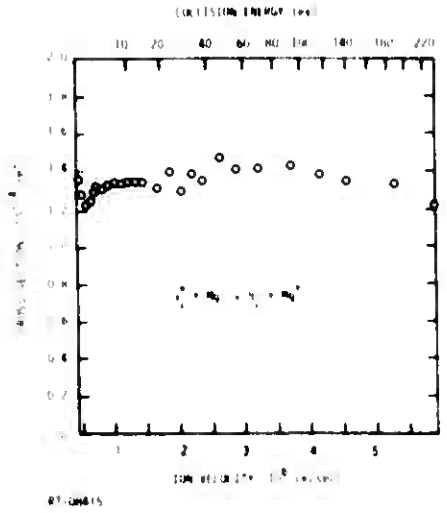

Figure 188-14. Cross-section for the reaction $N_2^+ + Mg \rightarrow N_2 + Mg^+$. Circles ere the date of Rutherford et el (Reference 188-6) obtained using crossed-beam techniques.

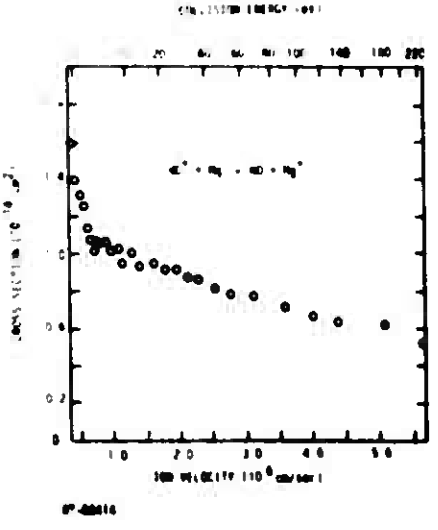

Figure 188 15 Cross-section for the reaction $NO^+ + Mg \rightarrow NO + Mg^+$ Circles are the date of Rutherford et al (Reference 188 6) obtained using crossed beam techniques.

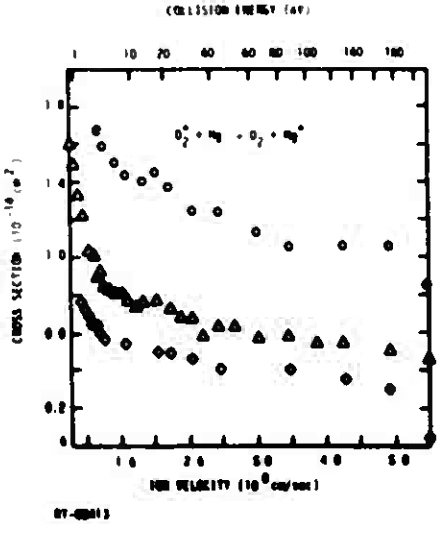

Figure 188 16 Cross-sections for the reaction $O_2^+ + Mg \rightarrow O_2 + Mg^+$. Diamonds are the rlate for ground-state O_2^+, circles are the data for metestable O_2^+, end triangles are the data for e composite beam of O_2^+ in which 32% of the O_2^+ is excited. All deta are from Rutherford et al (Reference 188-6) obtained using crossed-beam techniques.

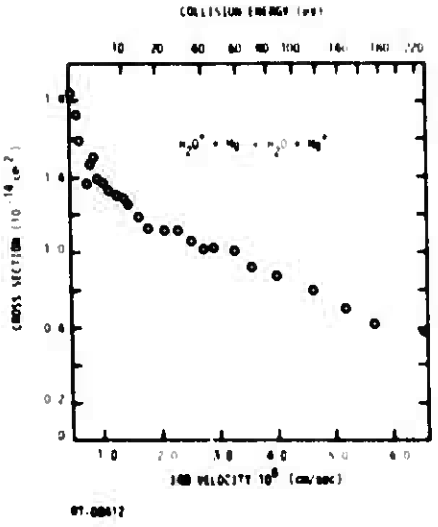

Figure 188-17. Cross-section for the reaction $H_2O^+ + Mg \rightarrow H_2O + Mg^+$. Circles are the data of Rutherford et al (Reference 188-6) obtained using crossed-beam techniques.

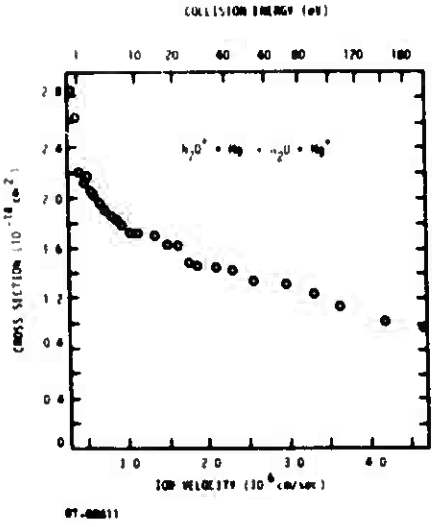

Figure 188-18. Cross-section for the reaction $N_2O^+ + Mg \rightarrow N_2O + Mg^+$. Circles are the data of Rutherford et al (Reference 188-6) obtained using crossed-beam techniques.

188.3.1.4 K-Atom Reactions

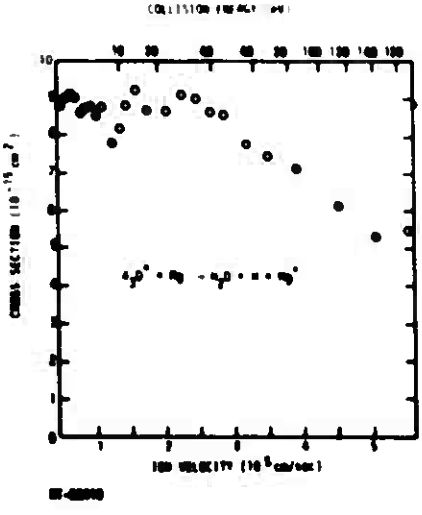

Figure 188-19. Cross-section for the reaction $H_3O^+ + Mg \rightarrow H_2O + H + Mg^+$. Circles are the data of Rutherford et al (Reference 188-6) obtained using crossed-beam techniques.

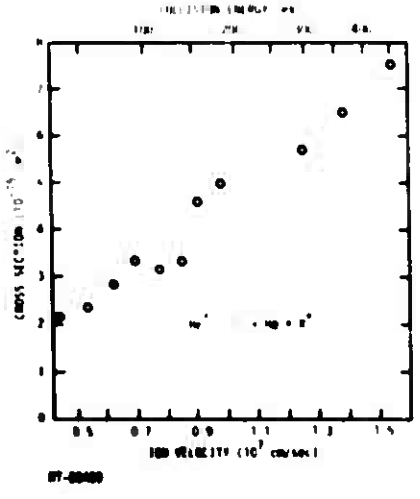

Figure 188-20. Cross-section for the reaction $He^+ + K \rightarrow He + K^+$. Circles are the data of Peterson and Lorents (Reference 188-17) obtained using crossed-beam techniques.

188.3.1.5 Co-Atom Reactions

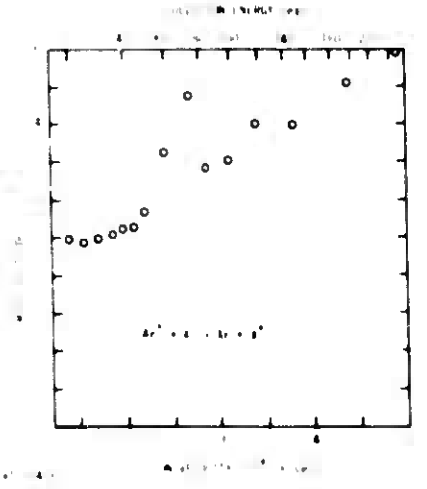

Figure 188-21 Cross section for the reaction $Ar^+ + K \rightarrow Ar + K^+$. Circles are the data of Peterson and Lorents (Reference 188 17) obtained using crossed-beam techniques

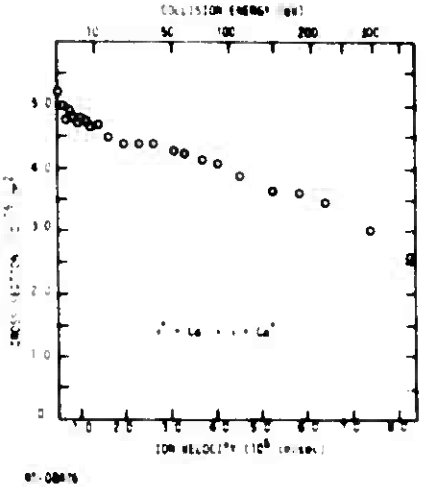

Figure 188-22 Cross section for the reaction $N^+ + Ca \rightarrow N + Ca^+$. Circles are the data of Rutherford et al (Reference 188 18) obtained using crossed-beam techniques

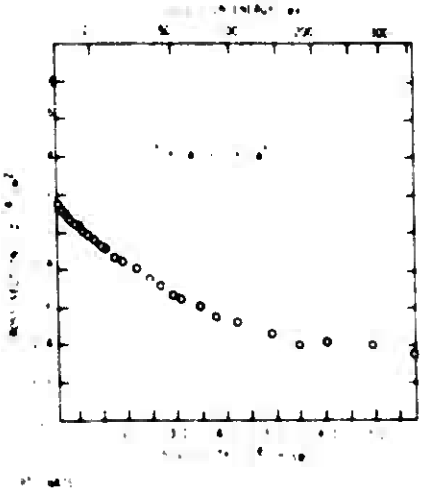

Figure 188 23 Cross section for the reaction $O^+ + Ca \rightarrow O + Ca^+$ Circles are the data of Rutherford et al (Reference 188 18) obtained using crossed beam techniques

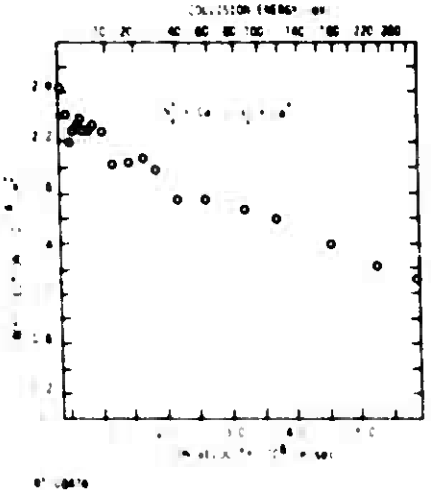

Figure 188 24 Cross section for the reaction $N_2^+ + Ca \rightarrow N_2 + Ca^+$ Circles are the data of Rutherford et al (Reference 188 18) obtained using crossed beam techniques.

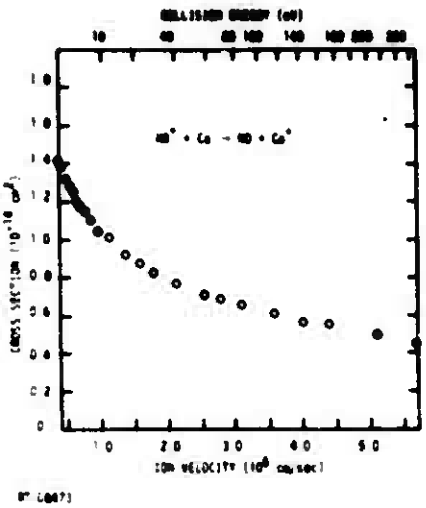

Figure 18B-25. Cross-section for the reaction $NO^+ + Ca \rightarrow NO + Ca^+$. Circles are the data of Rutherford et al (Reference 18B-18) obtained using crossed-beam techniques.

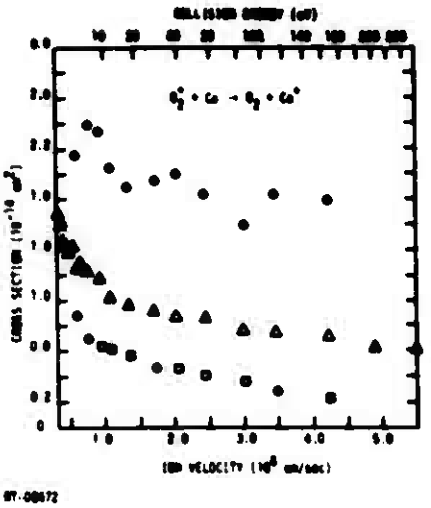

Figure 18B-26. Cross-sections for the reaction $O_2^+ + Ca \rightarrow O_2 + Ca^+$. Squares are the data for ground-state O_2^+, circles are the data for metastable O_2^+, and triangles are the data for a composite beam of O_2^+ in which 32% of the O_2^+ is excited. All data are from Rutherford et al (Reference 18B-18) obtained using crossed-beam techniques.

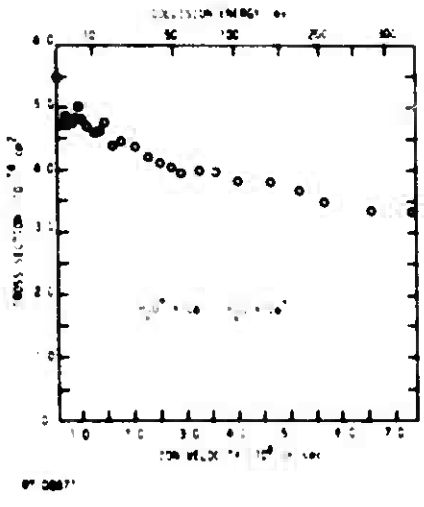

Figure 18B-27. Cross section for the reaction $H_2O^+ + Ca \rightarrow H_2O + Ca^+$. Circles are the data of Rutherford et al (Reference 18B-18) obtained using crossed-beam techniques.

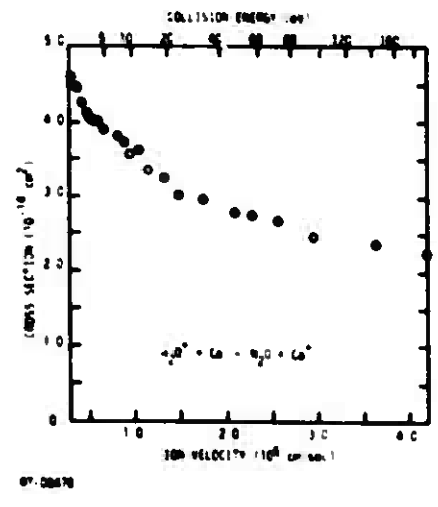

Figure 18B-28. Cross-section for the reaction $N_2O^+ + Ca \rightarrow N_2O + Ca^+$. Circles are the data of Rutherford et al (Reference 18B-18) obtained using crossed-beam techniques.

188.3.1.6 Fe-Atom Reactions

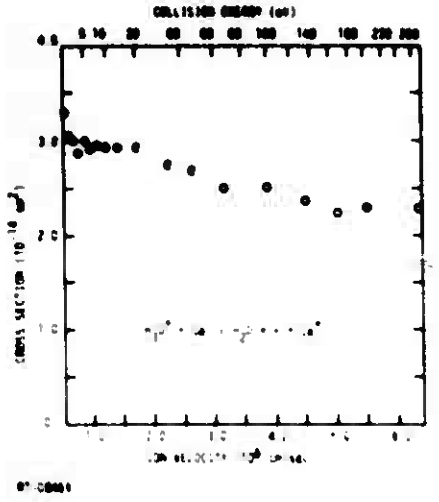

Figure 188-29 Cross section for the reaction $H_3O^+ + Ca \rightarrow H_2O + H + Ca^+$. Circles are the data of Rutherford et al (Reference 188-18) obtained using crossed beam techniques

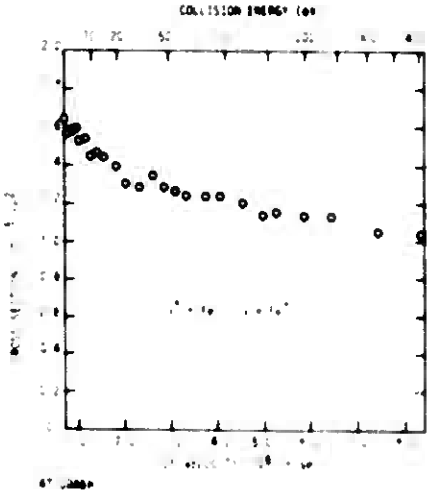

Figure 188-30 Cross section for the reaction $N^+ + Fe \rightarrow N + Fe^+$. Circles are the data of Rutherford and Vroom (Reference 188-19) obtained using crossed-beam techniques

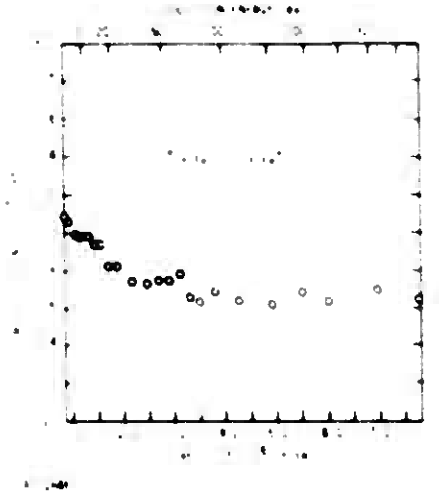

Figure 188-31 Cross section for the reaction $O^+ + Fe \rightarrow O + Fe^+$. Circles are the data of Rutherford and Vroom (Reference 188-19) obtained using crossed beam techniques

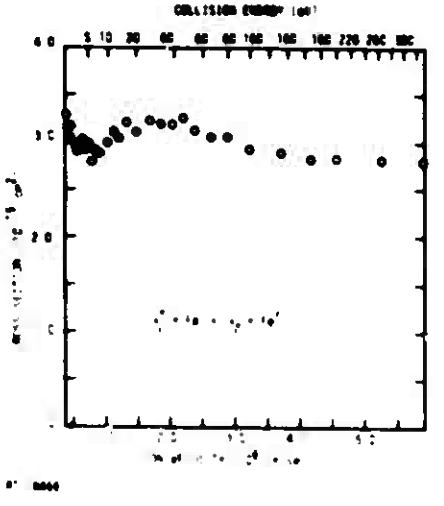

Figure 188-32 Cross section for the reaction $N_2^+ + Fe \rightarrow N_2 + Fe^+$. Circles are the data of Rutherford and Vroom (Reference 188-19) obtained using crossed beam techniques

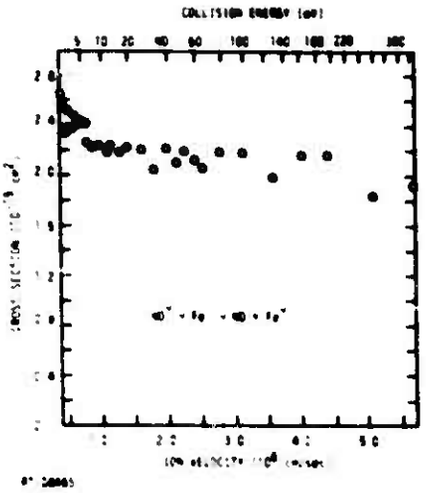

Figure 188-33. Cross-section for the reaction $NO^+ + Fe \rightarrow NO + Fe^+$. Circles are the data of Rutherford and Vroom (Reference 188-19) obtained using crossed-beam techniques.

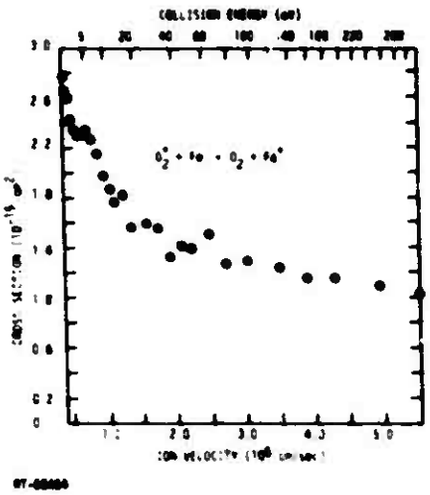

Figure 188-34. Cross-section for the reaction $O_2^+ + Fe \rightarrow O_2 + Fe^+$. Circles are the data of Rutherford and Vroom (Reference 188-19) obtained using crossed-beam techniques. No effects were seen due to metastable O_2^+ in the primary ion beam.

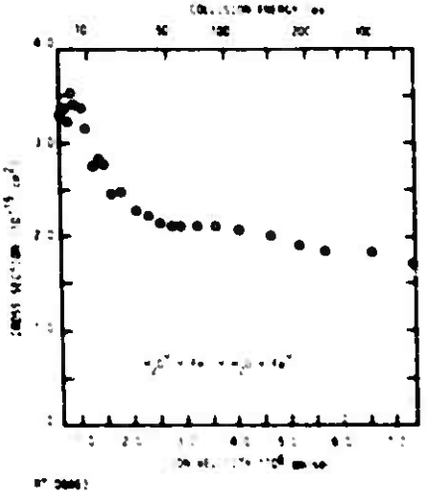

Figure 188-35. Cross-section for the reaction $H_2O^+ + Fe \rightarrow H_2O + Fe^+$. Circles are the data of Rutherford and Vroom (Reference 188-19) obtained using crossed-beam techniques.

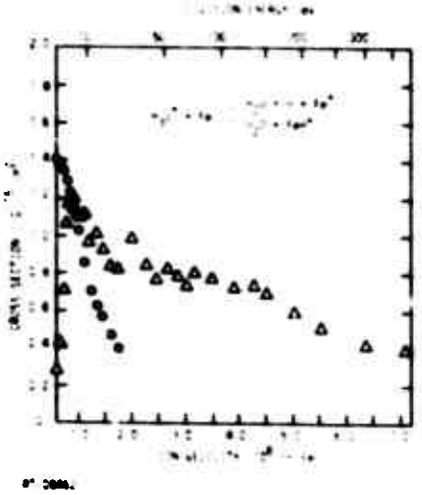

Figure 188-36. Cross-sections for the reactions $H_3O^+ + Fe \rightarrow H_2O + H + Fe^+$ and $H_3O^+ + Fe \rightarrow H_2O + FeH^+$. Triangles are the data for formation of the Fe^+ product and circles are the data for formation of FeH^+. All data are from Rutherford and Vroom (Reference 188-19) obtained using crossed-beam techniques.

...tions

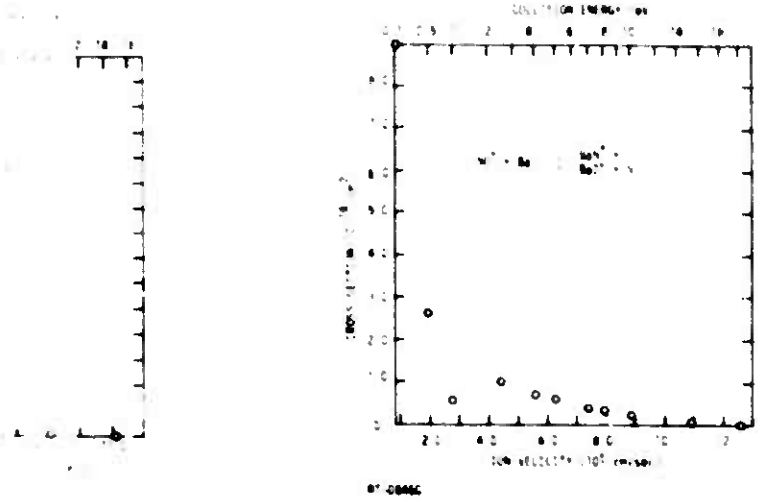

Ba + Baf_2 + N
al (Reference
ams techniques
ergy electron

Figure 188 38 Composite cross section for the reactions $NO^+ + Ba \rightarrow BaN^+ + O$ and $NO^+ + Ba \rightarrow BaO^+ + N$. Circles are the data of Neynaber et al (Reference 188 20) obtained using merging beams techniques. The NO^+ was produced using low energy electron impact

188.3.1.8 N_2-Molecule Reactions

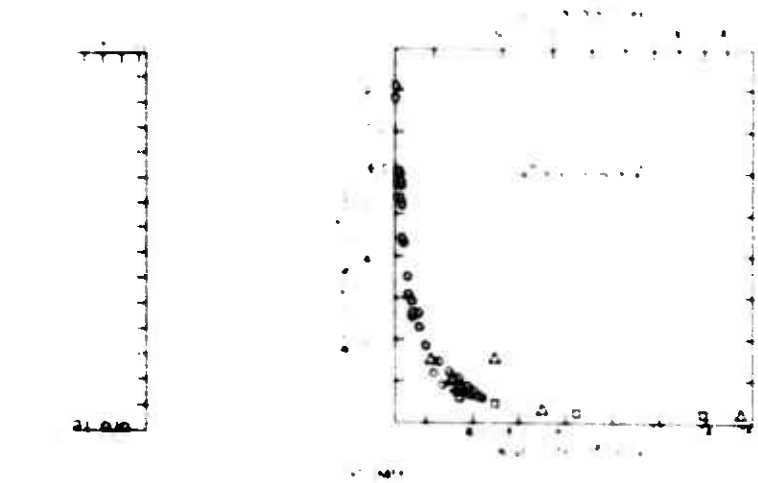

Ba + BaO^+ + O
al (Reference
ams techniques
ergy electron

Figure 188 40 Cross section for the reaction $He^+ + N_2 \rightarrow He + N_2^+$. Circles are the data of Meier (Reference 188 21) obtained using beam-gas cell techniques, triangles are the data of Stebbings, Rutherford, and Turner (Reference 188 22) obtained using crossed beam techniques, and squares are the data of Gustafsson and Lindholm (Reference 188 23) obtained using beam-gas cell techniques

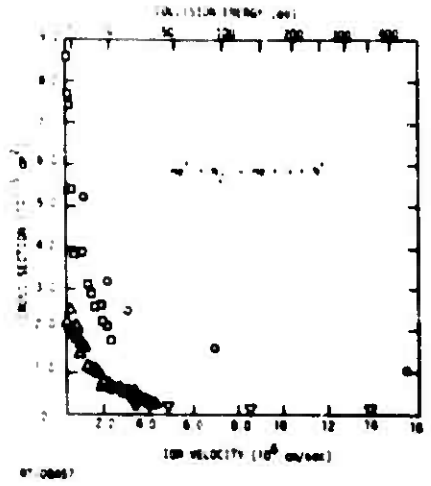

Figure 188-41 Cross section for the reaction $He^+ + N_2 \rightarrow He + N + N^+$. Triangles (apex up) are the data of Maier (Reference 188-21) obtained using beam-gas cell techniques, circles are the data of Stebbings, Rutherford, and Turner (Reference 188-22) obtained using crossed-beam techniques, triangles (apex down) are the data of Gustafsson and Lindholm (Reference 188-23) obtained using beam-gas cell techniques, and squares are the data of Moran and Friedman (Reference 188-24) obtained using ion source techniques.

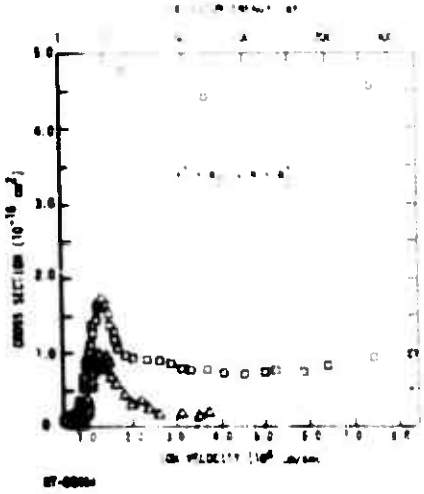

Figure 188-42. Cross section for the reaction [illegible]. Triangles are the data of Maier and Morac (Reference 188-25) obtained using beam-gas cell techniques, squares are the data of Neynaber, Rutherford, and Vroom (Reference 188-26) obtained using crossed-beam techniques, and circles are the data of Stebbings, Turner, and Smith (Reference 188-27) obtained using a beam-gas cell technique in which all the slow ions formed are collected.

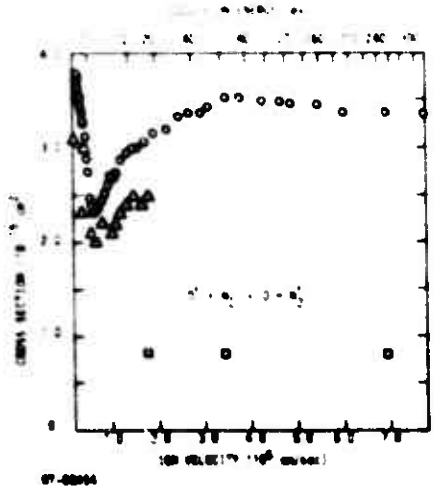

Figure 188-43 Cross section for the reaction $O^+ + N_2 \rightarrow O + N_2^+$. Note that the O^+ must be in a metastable state to make the reaction proceed at low energies. Circles are the data of Rutherford and Vroom (Reference 188-28) obtained using crossed-beam techniques. The data are corrected for the amount of metastable O^+ in the beam. Triangles are the data of Tiernan (Reference 188-29) obtained using beam-gas cell techniques. The data are corrected for the amount of metastable O^+ in the beam. Squares are the data of Stebbings, Turner, and Smith (Reference 188-27) obtained using a beam-gas cell technique in which all slow ions are collected. No correction for the composition of the beam is made.

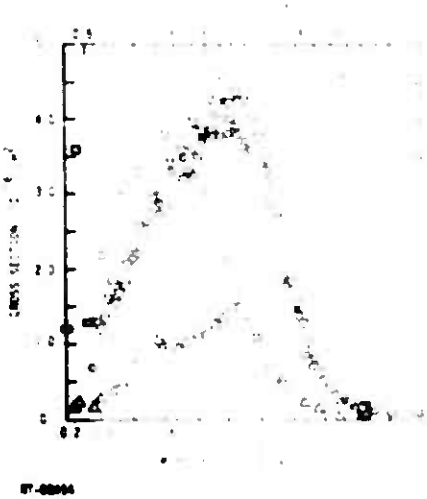

Figure 188-44 [illegible]

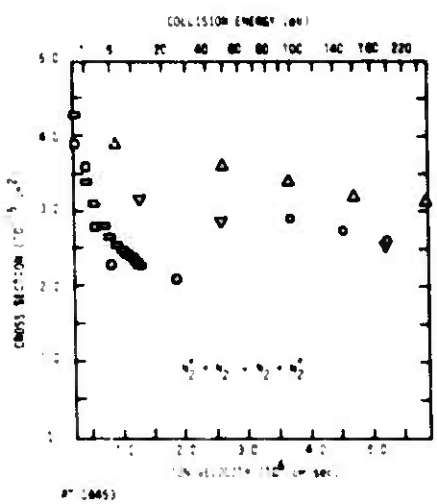

Figure 18B-45. Cross-section for the reaction $N_2^+ + N_2 \rightarrow N_2 + N_2^+$. Flat rectangles are the data of Moren and Roberts (Reference 18B-32) obtained using a modified ion source technique, circles are the data of Neff (Reference 18B-33) obtained using a beam-gas cell system in which all slow ions are collected, squares are the data of Leventhal, Moran, and Friedman (Reference 18B-34) obtained using a beam-gas cell technique, triangles (apex up) are the data of Amme and Utterback (Reference 18B-35) obtained using a beam-gas cell technique in which slow ions are collected, and triangles (apex down) are the data of Stebbings, Turner, and Smith (Reference 18B-27) obtained using a beam-gas cell technique in which [illegible] ions are collected.

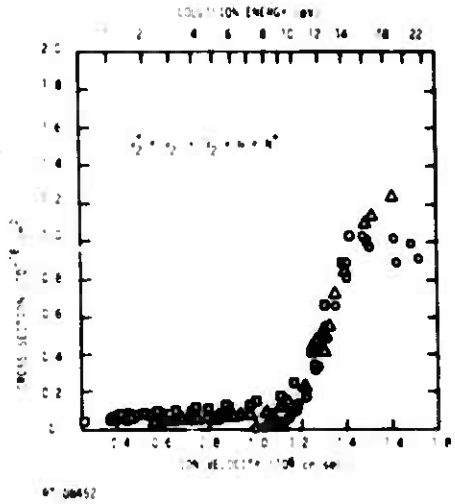

Figure 18B-46. Cross-section for the reaction $N_2^+ + N_2 \rightarrow N_2 + N + N^+$. Circles are the data for N_2^+ formed by 19.3 eV electrons, squares are the data for N_2^+ formed by 25.5 eV electrons, and triangles are the data for N_2^+ formed by 57.0 eV electrons. The data are from Meier (Reference 18B-3E) obtained using beam-gas cell techniques.

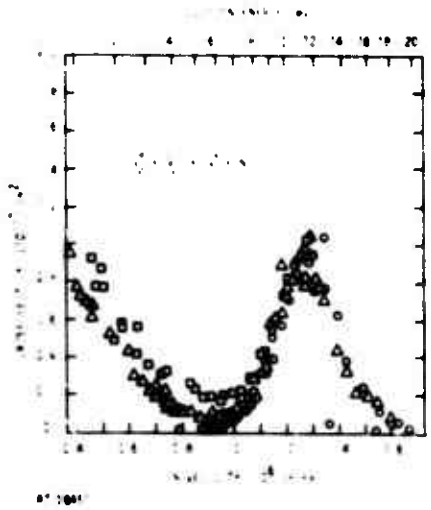

Figure 18B-47. Cross-section for the reaction $N_2^+ + N_2 \rightarrow N_3^+ + N$. Circles are the data for N_2^+ formed by 19 eV electrons, squares are the data for N_2^+ formed by 25.5 eV electrons, and triangles are the data for N_2^+ formed by 57 eV electrons. The data are from Meier (Reference 18B-36) obtained using beam-gas cell techniques

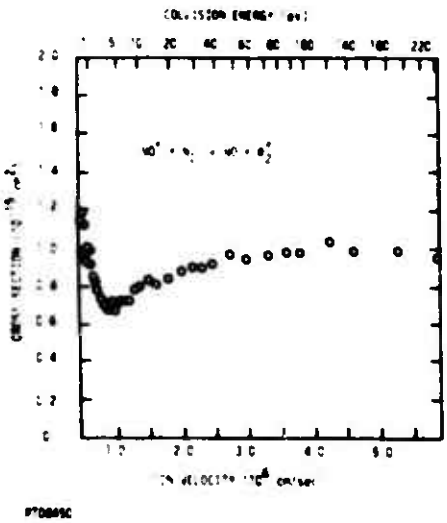

Figure 18B-48. Cross-section for the reaction $NO^+ + N_2 \rightarrow NO + N_2^+$. Note that the NO^+ must be in a metastable state to make the reaction proceed at low energies. Circles are the data of Neynaber, Rutherford, and Vroom (Reference 18B-26) obtained using crossed-beam techniques. The cross-sections are corrected for the fraction of metastable ions present in the beam.

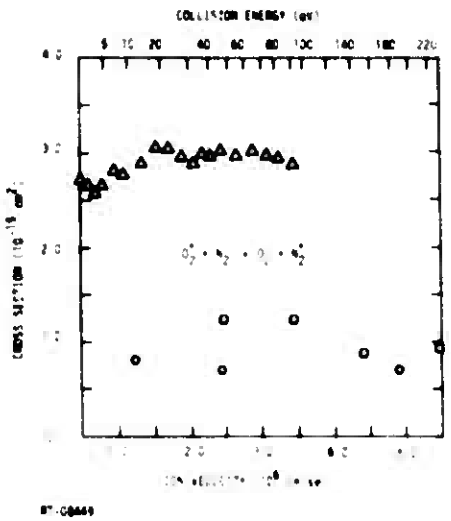

Figure 188-49. Cross section for the reaction $O_2^+ + N_2 \rightarrow O_2 + N_2^+$. Note that the O_2^+ must be in a metastable state to make the reaction proceed at low energies. Triangles are the data of Rutherford (Reference 188-37) obtained using crossed beam techniques. These data are corrected for the fraction of metastable ions present in the beam. Circles are the data of Amme and Utterback (Reference 188-35), and squares are the data of Stebbings, Turner, and Smith (Reference 188-27). Both of the latter sets of data were obtained with beam gas cell techniques using slow-ion collection, and neither is corrected for the excited states in the beam.

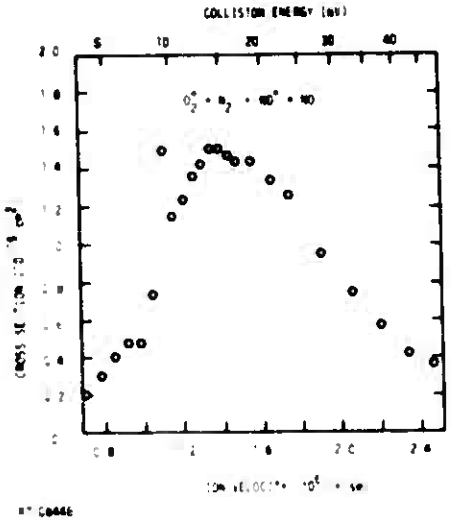

Figure 188-50. Cross section for the reaction $O_2^+ + N_2 \rightarrow NO^+ + NO$. Circles are the data of Rutherford (Reference 188-37) obtained using crossed-beam techniques.

188.3.1.9 NO-Molecule Reactions

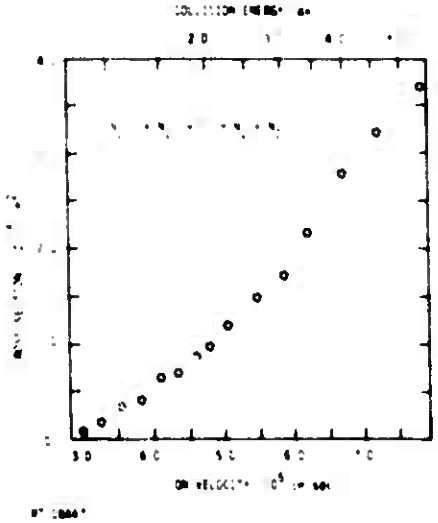

Figure 188-51. Cross section for the reaction $N_2O^- + N_2 \rightarrow O^- + N_2 + N_2$. Circles are the data of Tiernan and Clow (Reference 188-38) obtained using beam-gas cell techniques.

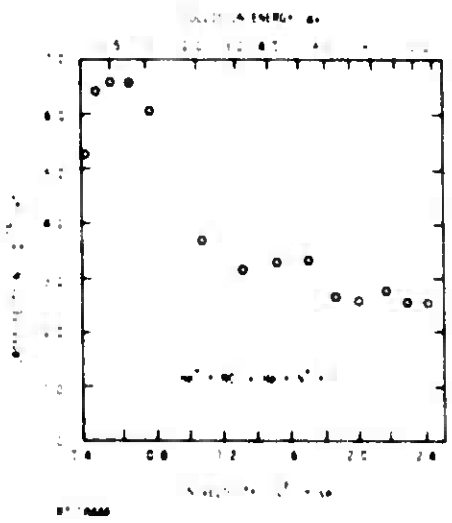

Figure 188-52. Cross section for the reaction $He^+ + NO \rightarrow He + N^+ + O$. Circles are the data of Moran and Friedman (Reference 188-24) obtained using ion-source techniques.

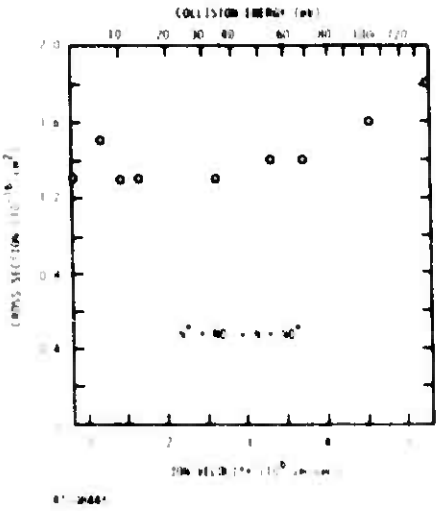

Figure 188-53. Cross-section for the reaction $N^+ + NO \rightarrow N + NO^+$. Circles are the data of Turner, Rutherford, and Stebbings (Reference 188-39) obtained using crossed-beam techniques.

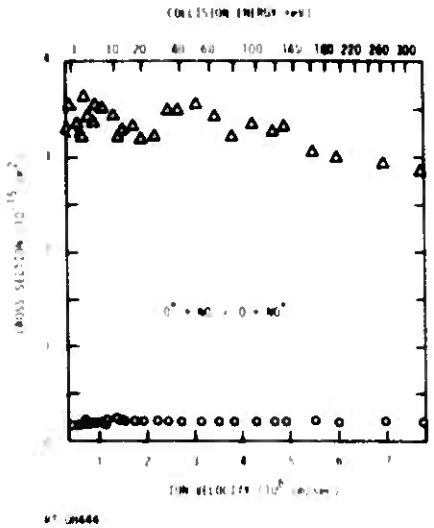

Figure 188-54. Cross-sections for the reaction $O^+ + NO \rightarrow O + NO^+$. Triangles are the data for metastable O^+ ions and circles are the data for ground-state ions. All data are from Rutherford (Reference 188-37) and were obtained using crossed-beam techniques.

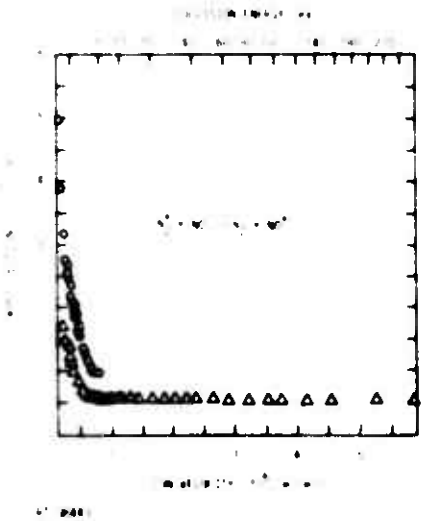

Figure 188-55. Cross-section for the reaction $N_2 + NO \rightarrow N_2 + NO^+$. Circles are the data of Paulson (Reference 188-30) obtained using beam-gas cell techniques, and triangles are the data of Neynaber, Rutherford, and Vroom (Reference 188-26) obtained using crossed-beam techniques. The excess energy in this reaction is such that either the NO^+ or the N_2 product may be left in an excited state.

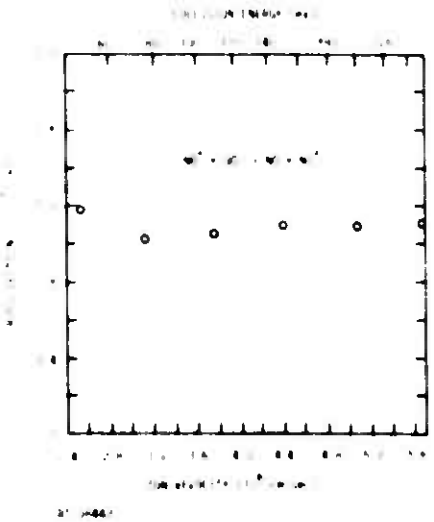

Figure 188-56. Cross-section for the reaction $NO^+ + NO \rightarrow NO + NO^+$. Circles are the data of Ghosh and Sheridan (Reference 188-40) obtained using beam-gas cell techniques.

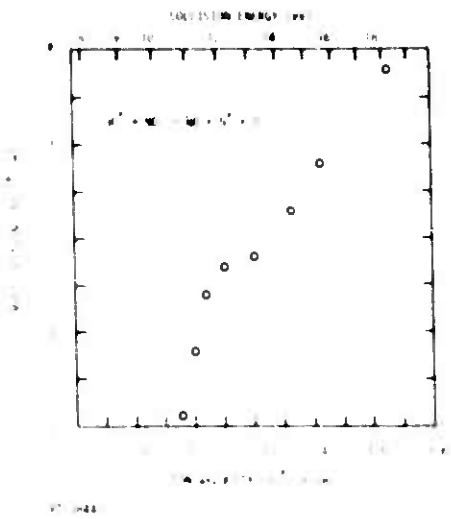

Figure 188 57 Cross section for the reaction $NO^+ + NO \rightarrow NO + N^+ + O$. Circles are the data of Moran and Roberts (Reference 188 32) obtained using a modified ion-source technique

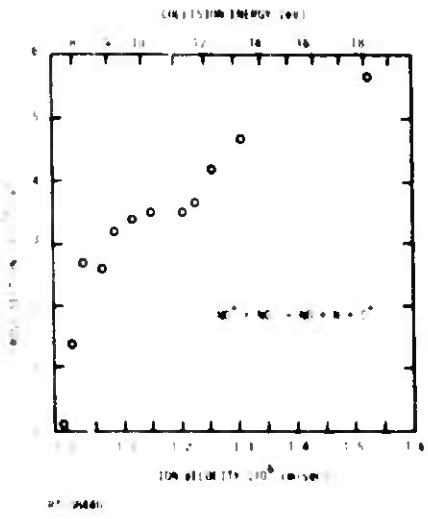

Figure 188 58 Cross section for the reaction $NO^+ + NO \rightarrow NO + N + O^+$ Circles are the data of Moran and Roberts (Reference 188 32) obtained using a modified ion-source technique

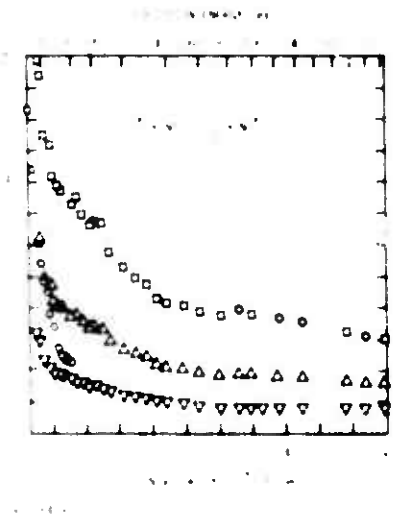

Figure 188 59 Cross sections for the reaction $O_2^+ + NO \rightarrow O_2 + NO^+$ Circles are the data of Paulson (Reference 188 30) obtained using beam-gas techniques with a mixed beam. Squares are the data for metastable O_2^+, triangles (apex down) are the data for a ground state beam, and triangles (apex up) are the data for a composite beam, all three sets of data coming from Rutherford (Reference 188 37) and obtained using crossed-beam techniques

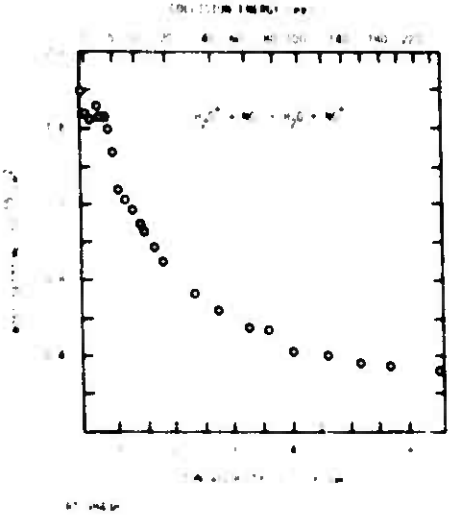

Figure 188 60 Cross section for the reaction $H_2O^+ + NO \rightarrow H_2O + NO^+$ Circles are the data of Turner and Rutherford (Reference 188 41) obtained using crossed-beam techniques

188.3.1.10 O_2-Molecule Reactions

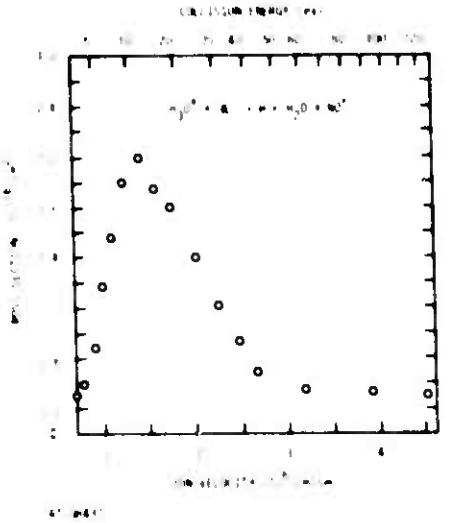

Figure 188-61 Cross-section for the reaction $H_3O^+ + NO \rightarrow H + H_2O + NO^+$. Circles are the data of Turner and Rutherford (Reference 188-41) obtained using crossed-beam techniques.

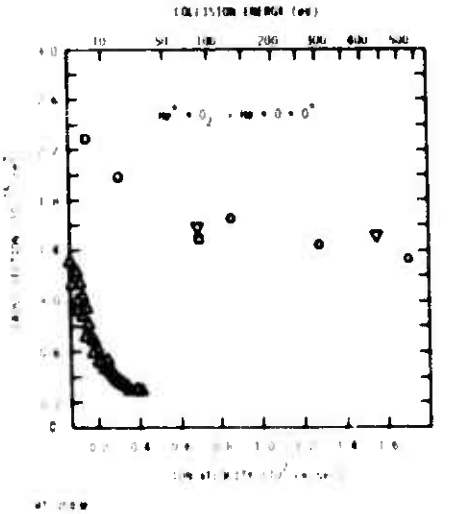

Figure 188-62. Cross-section for the reaction $He^+ + O_2 \rightarrow He + O + O^+$. Triangles (apex up) are the data of Maier (Reference 188-21) obtained using beam-gas cell techniques, circles are the data of Fite et al (Reference 188-42) obtained using crossed-beam techniques with slow-ion measurements, squares are the data of Stebbings, Rutherford, and Turner (Reference 188-22) obtained using crossed-beam techniques, and triangles (apex down) are the data of Utterback and Amme (Reference 188-43) obtained using a beam-gas cell technique with slow-ion collection.

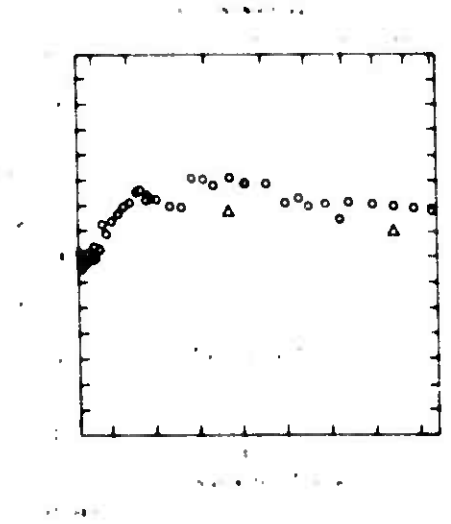

Figure 188-63 Cross-section for the reaction $N^+ + O_2 \rightarrow N + O_2^+$. Circles are the data of Neynaber, Rutherford, and Vroom (Reference 188-44) obtained using crossed-beam techniques, and triangles are the data of Stebbings, Turner, and Smith (Reference 188-27) obtained using beam-gas cell techniques with total slow-ion collection.

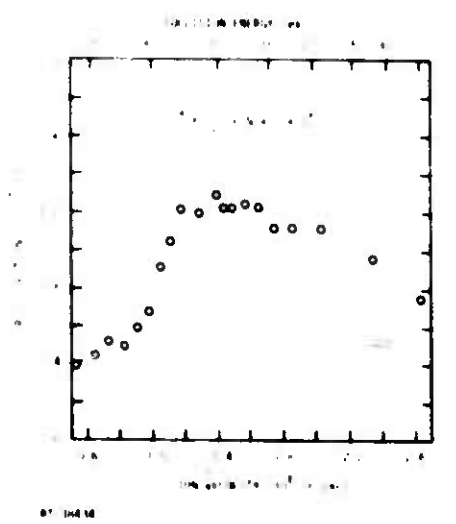

Figure 188-64. Cross-section for the reaction $N^+ + O_2 \rightarrow N + O + O^+$. Circles are the data of Neynaber, Rutherford, and Vroom (Reference 188-44) obtained using crossed-beam techniques.

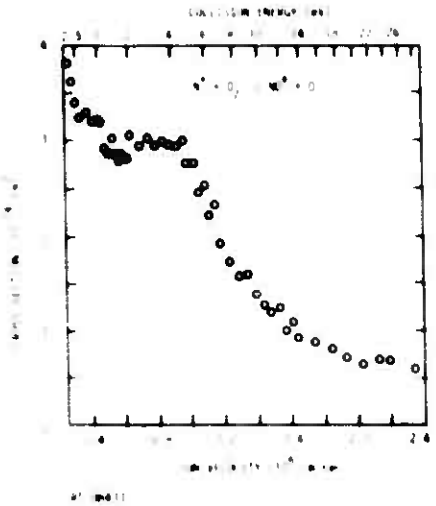

Figure 18B 65 Cross section for the reaction $N^+ + O_2 \rightarrow NO^+ + O$ Circles are the data of Neynaber, Rutherford, and Vroom (Reference 18B 44) obtained using crossed-beam techniques

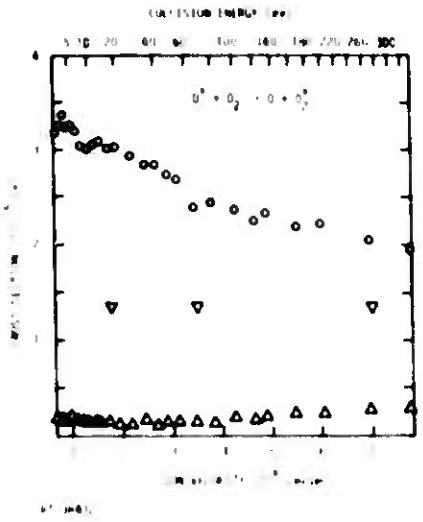

Figure 18B 66 Cross sections for the reaction $O^+ + O_2 \rightarrow O + O_2^+$. Circles are the data for metastable O^+ ions and triangles (apex up) are the data for ground-state ions. Both sets of data are from Rutherford (Reference 18B 37) obtained using crossed-beam techniques. Triangles (apex down) are the data of Stebbings, Turner, and Smith (Reference 18B 27) obtained using crossed-beam techniques and slow-ion collection. No state selection of the primary beam was used

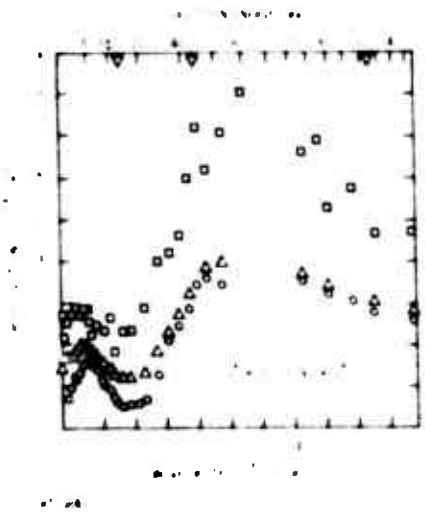

Figure 18B 67 Cross section for the reaction $N_2^+ + O_2 \rightarrow N_2 + O_2^+$. Circles are the data for both reactants having a minimum of internal energy, squares are the data for N_2^+ having minimum internal energy and O_2 heated to 1600 K, and triangles (apex up) are the data for N_2^+ formed by 40 eV electrons and O_2 having minimum internal energy. All three sets of data are from Neynaber, Rutherford, and Vroom (Reference 18B 44) obtained using crossed-beam techniques. Triangles (apex down) are the data of Stebbings, Turner, and Smith (Reference 18B 27) obtained using crossed-beam techniques with slow-ion collection

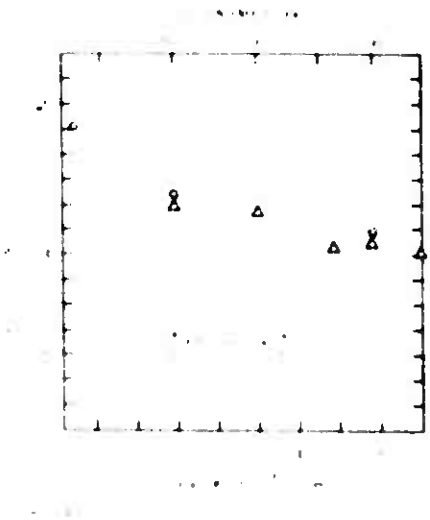

Figure 18B 68 Cross section for the reaction $O_2^+ + O_2 \rightarrow O_2 + O_2^+$. Triangles are the data of Aitme and Utterback (Reference 18B 35) obtained using beam-gas cell techniques with total slow-ion collection, and circles are the data of Stebbings, Turner, and Smith (Reference 18B 27) obtained using crossed-beam techniques with slow-ion collection.

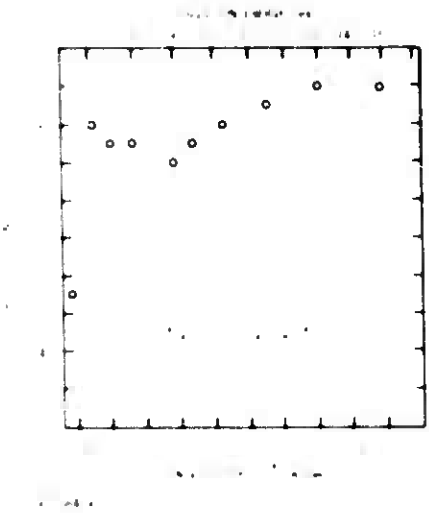

Figure 18B 69 Cross section for the reaction $O_2^+ + O_2 \rightarrow O_2 + O + O^+$ Circles are the data of Moran and Roberts (Reference 18B 32) obtained using a modified ion source experiment

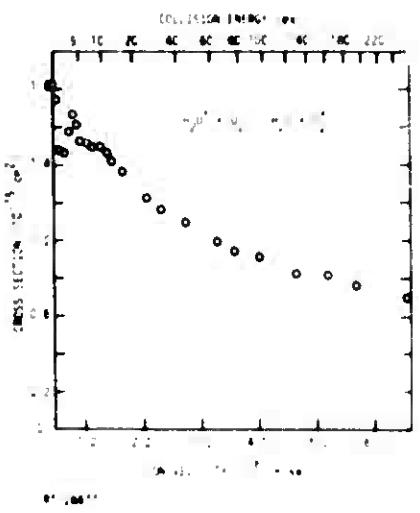

Figure 18B 70 Cross-section for the reaction $H_2O^+ + O_2 \rightarrow H_2O + O_2^+$ Circles are the data of Turner and Rutherford (Reference 18B-41) obtained using crossed-beam techniques

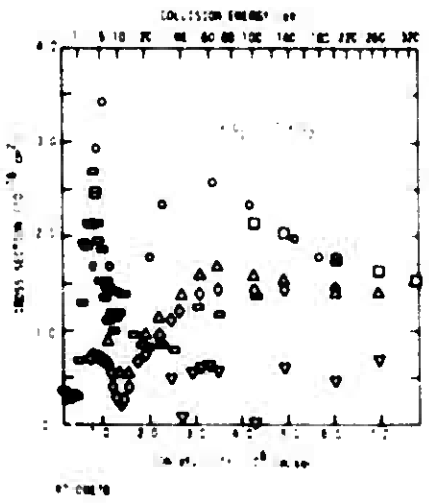

Figure 18B 71 Cross sections for the reaction $O^- + O_2 \rightarrow O + O_2^-$ Flat rectangles are the data of Paulson (Reference 18B 45) obtained using beam gas cell techniques, circles are the data of Bailey and Mahadevan (Reference 18B 46) obtained using a beam-gas cell technique with slow ion collection, squares are the data of Snow, Rundel, and Geballe (Reference 18B-47) obtained using crossed beam techniques, triangles (apex up) are the data for a ground state O_2 target and triangles (apex down) are the data for a metastable O_2 target from Mathis (Reference 18B 48) obtained using crossed beam techniques, and diamonds are the data of Rutherford and Turner (Reference 18B 49) obtained using crossed-beam techniques

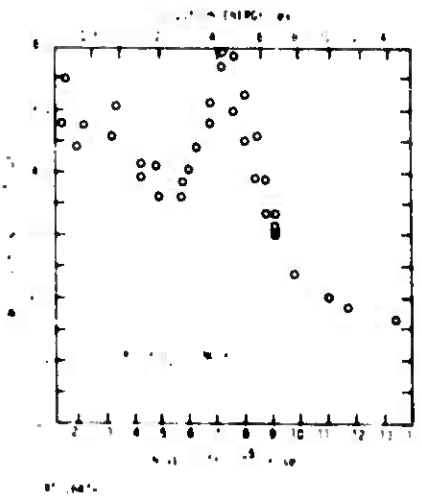

Figure 18B 72 Cross-section for the reaction $NO^- + O_2 \rightarrow NO + O_2^-$ Circles are the data of Paulson (Reference 18B-30) obtained using beam-gas cell techniques

18B.3.1.11 H_2O-Molecule Reactions

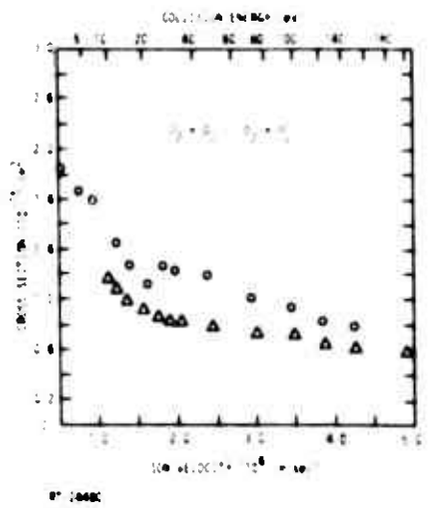

Figure 18B-73 Cross-section for the reaction $O_2^- + O_2 \rightarrow O_2 + O_2^-$ Triangles are the data of Rutherford and Turner (Reference 18B-49) obtained using crossed-beam techniques, and circles are the data of Bailey and Mahadevan (Reference 18B-46) obtained using a beam-gas cell technique with slow-ion collection.

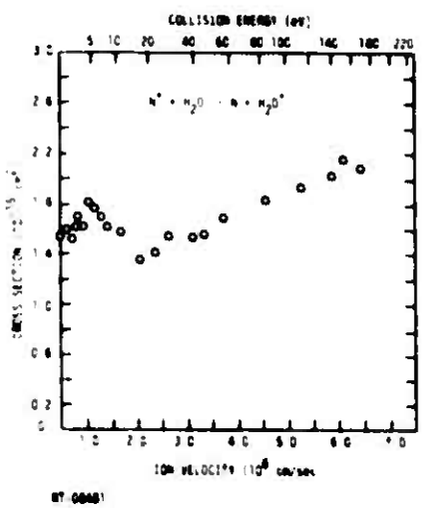

Figure 18B-74. Cross-section for the reaction $N^+ + H_2O \rightarrow N + H_2O^+$ Circles are the data of Turner and Rutherford (Reference 18B-41) obtained using crossed-beam techniques

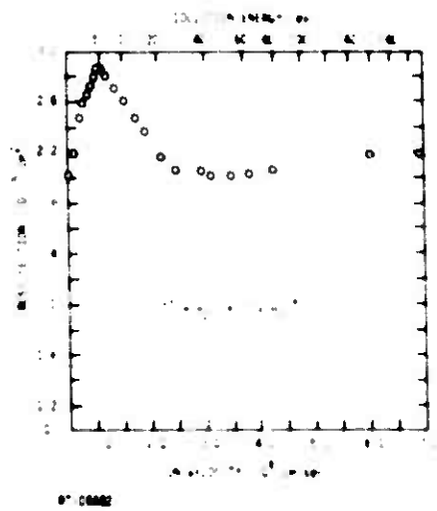

Figure 18B-75 Cross section for the reaction $O^+ + H_2O \rightarrow O + H_2O^+$ Circles are the data of Turner and Rutherford (Reference 18B-41) obtained using crossed-beam techniques

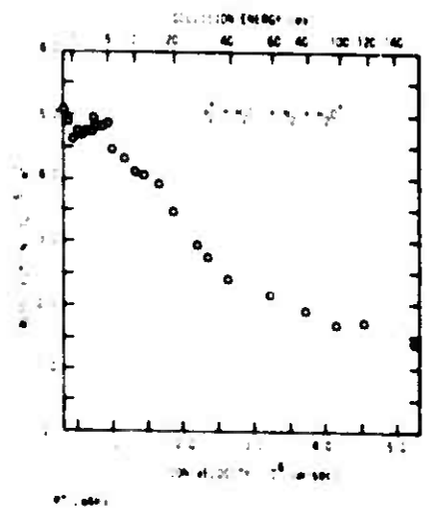

Figure 18B-76. Cross-section for the reaction $N_2^+ + H_2O \rightarrow N_2 + H_2O^+$ Circles are the data of Turner and Rutherford (Reference 18B-41) obtained using crossed-beam techniques

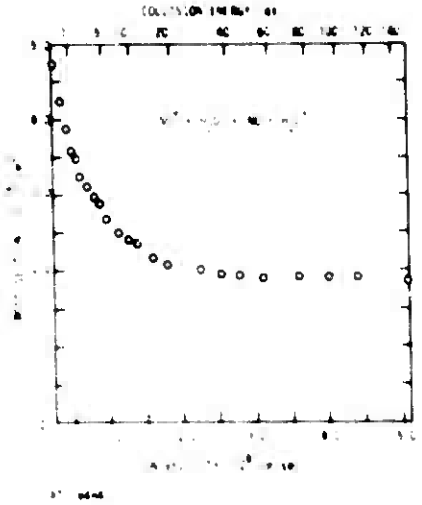

Figure 188 77 Cross section for the reaction $NO^+ + H_2O \rightarrow NO + H_2O^+$ Note thet the NO^+ must be in a metastable state for the reaction to proceed at low energies. Circles are the data of Turner and Rutherford (Reference 188 41) obtained using crossed beam techniques The data are corrected for the fraction of metastable ions in the beam

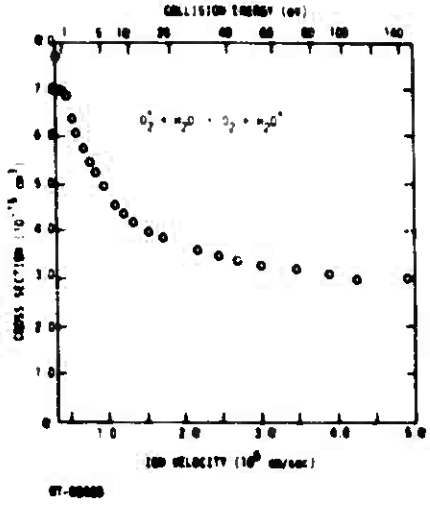

Figure 188 78 Cross section for the reaction $O_2^+ + H_2O \rightarrow O_2 + H_2O^+$ Note that the O_2^+ must be in a metastable state for the reaction to proceed at low energies. Circles ere the deta of Turner and Rutherford (Reference 188 41) obtained using crossed beam techniques The data are corrected for the fraction of metastable ions in the beam

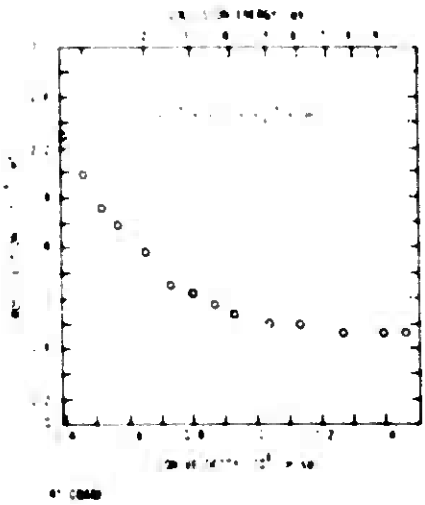

Figure 188 79 Cross section for the reaction $H_2O^+ + H_2O \rightarrow H_3O^+ + OH$ Circles are the data of Turner end Rutherford (Reference 188 41) obtained using crossed beam techniques

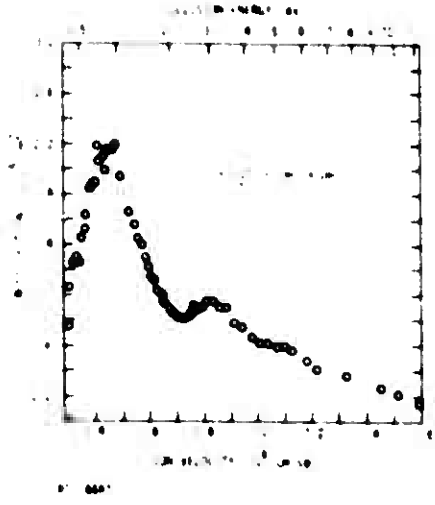

Figure 188 80 Cross section for the reaction $O^- + H_2O \rightarrow OH^- + OH$ Circles are the data of Paulson (Reference 188-30) obtained using beam gas cell techniques

18B.3.1.12 N_2O-Molecule Reactions

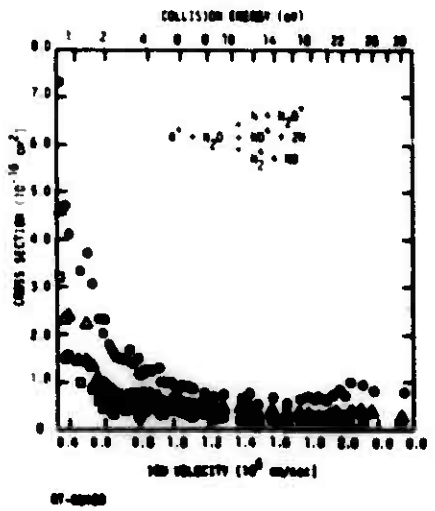

Figure 18B-81. Cross-sections for the reactions $N^+ + N_2O \rightarrow N + N_2O^+$ (circles), $N^+ + N_2O \rightarrow NO^+ + N + N$ (triangles), and $N^+ + N_2O \rightarrow N_2^+ + NO$ (squares). All data are from Murad (Reference 18B-50) obtained using beam-gas cell techniques.

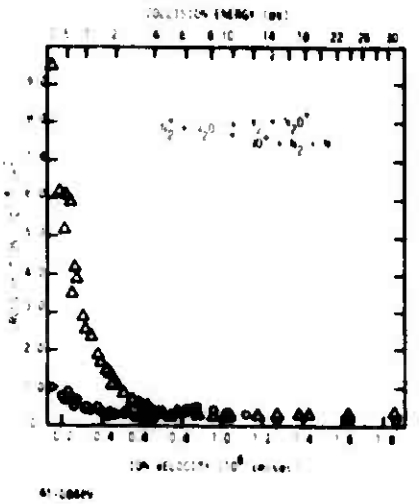

Figure 18B-82. Cross sections for the reactions $N_2^+ + N_2O \rightarrow N_2 + N_2O^+$ (triangles) and $N_2^+ + N_2O \rightarrow NO^+ + N_2 + N$ (circles). All data are from Murad (Reference 18B-50) obtained using beam-gas cell techniques.

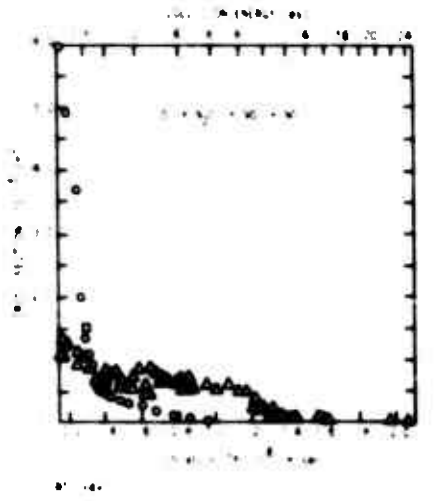

Figure 18B-83. Cross-section for the reaction $O^- + N_2O \rightarrow NO^- + NO$. Circles are the data of Tiernan and Clow (Reference 18B-38) obtained using beam-gas cell techniques, triangles are the data of Paulson (Reference 18B-51) obtained using beam-gas cell techniques, and the square is the datum of Stockdale, Compton, and Reinhardt (Reference 18B-52) obtained using ions produced by dissociative attachment.

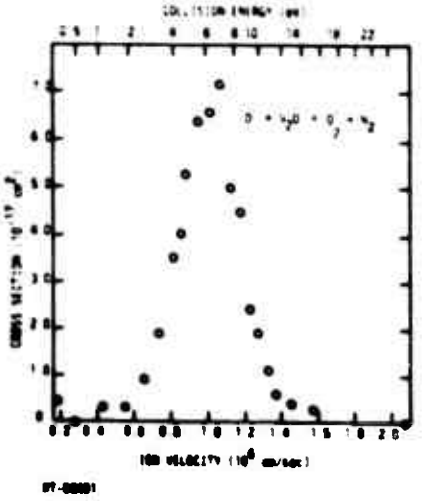

Figure 18B-84. Cross-section for the reaction $O^- + N_2O \rightarrow O_2^- + N_2$. Circles are the data of Paulson (Reference 18B-51) obtained using beam-gas cell techniques.

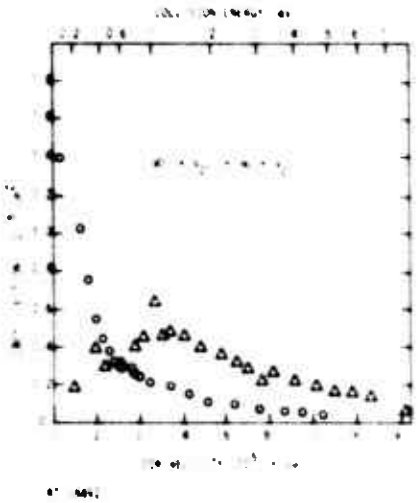

Figure 188 85 Cross section for the reaction $NO^- + N_2O \rightarrow NO + N_2O^-$ Triangles are the data of Paulson (Reference 188 51) and circles are the data of Tiernan and Clow (Reference 188 38), both obtained using beam gas cell techniques

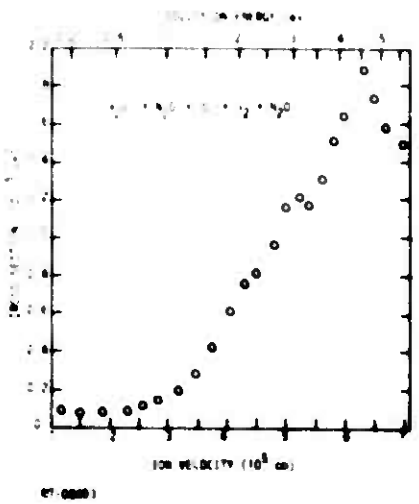

Figure 188 86 Cross section for the reaction $N_2O^- + N_2O \rightarrow O^- + N_2 + N_2O$ Circles are the data of Tiernan and Clow (Reference 188 38) obtained using beam gas cell techniques

188.3.1.13 CO_2-Molecule Reactions

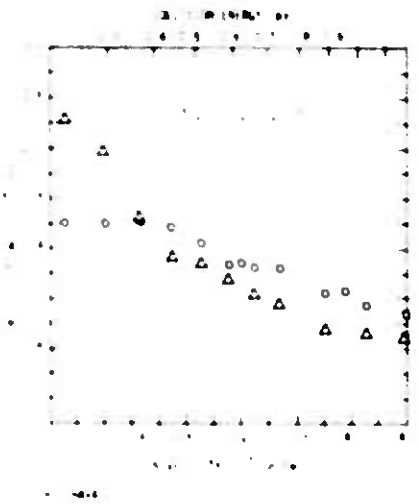

Figure 188 87 Cross sections for the reaction $O^- + CO_2 \rightarrow O + CO_2^-$ Circles are the data for ground state O^- and triangles are the data for excited state O^- All data are from Tiernan (Reference 188 29) obtained using beam gas cell techniques

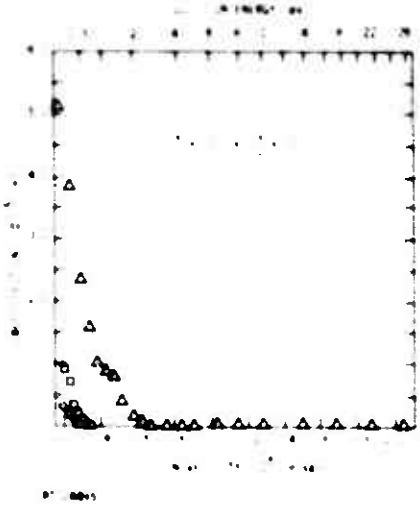

Figure 188 88 Cross sections for the reaction $O^- + CO_2 \rightarrow O_2^- + CO$ Triangles are the data of Paulson (Reference 188 30) obtained using beam-gas cell techniques. Squares and circles are the data of Tiernan (Reference 188 29) for ground state and excited O^- ions, respectively, obtained using beam gas cell techniques

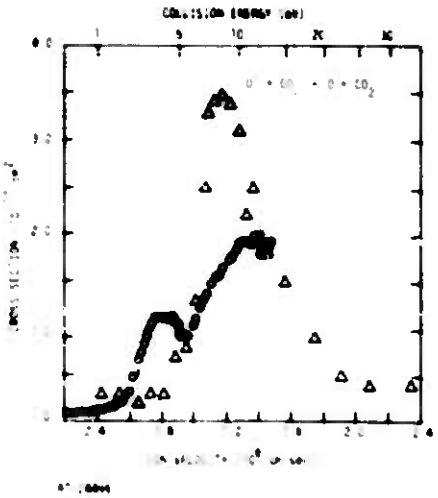

Figure 188-89. Cross-section for the reaction $O^- + CO_2 \rightarrow O + CO_2^-$. Circles are the data of Tiernan and Clow (Reference 188-38) and triangles are the data of Paulson (Reference 188-51), both obtained using beam-gas cell techniques.

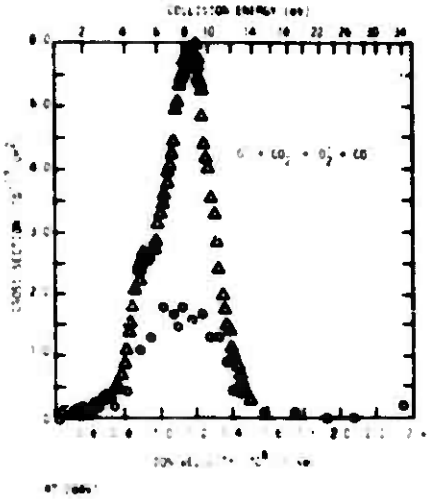

Figure 188-90. Cross-section for the reaction $O^- + CO_2 \rightarrow O_2^- + CO$. Triangles are the data of Tiernan and Clow (References 188-38) and circles are the data of Paulson (Reference 188-51), both obtained using beam-gas cell techniques.

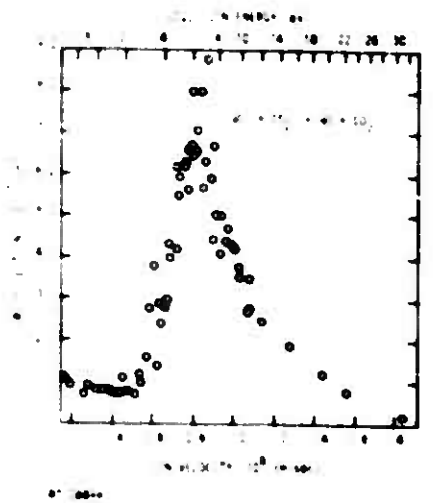

Figure 188-91. Cross-section for the reaction $NO^- + CO_2 \rightarrow NO + CO_2^-$. Circles are the data of Paulson (Reference 188-53) obtained using beam-gas cell techniques.

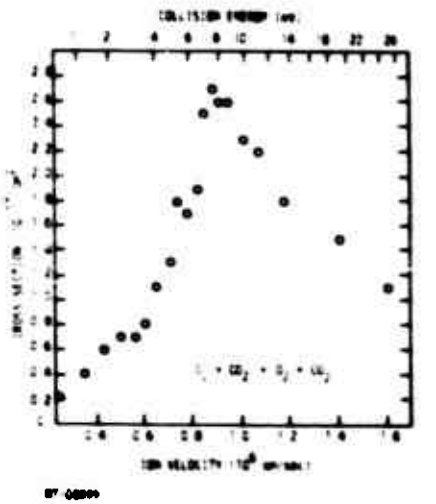

Figure 188-92. Cross-section for the reaction $O_2^- + CO_2 \rightarrow O_2 + CO_2^-$. Circles are the data of Paulson (Reference 188-53) obtained using beam-gas cell techniques.

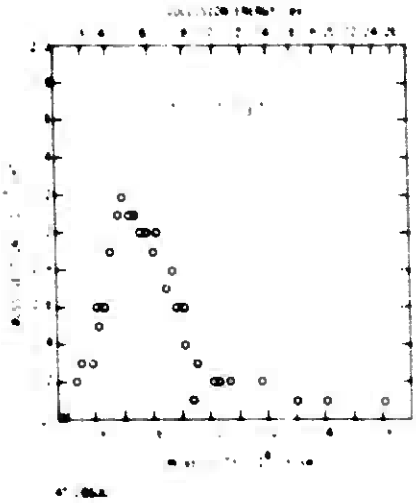

Figure 188 93 Cross section for the reaction $O_2^- + CO_2 \rightarrow CO_3^- + O$ Circles are the data of Paulson (Reference 188 53) obtained using beam gas cell techniques

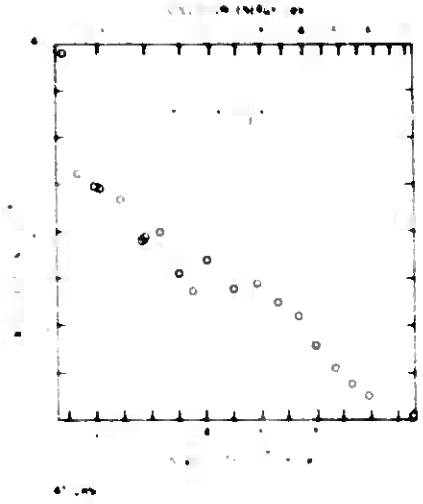

Figure 188 94 Cross section for the reaction $O_3^- + CO_2 \rightarrow CO_3^- + O_2$ Circles are the data of Neynaber, Rutherford, and Vroom (Reference 188 54) obtained using crossed beam techniques

188.3.1.14 NO_2-Molecule Reactions

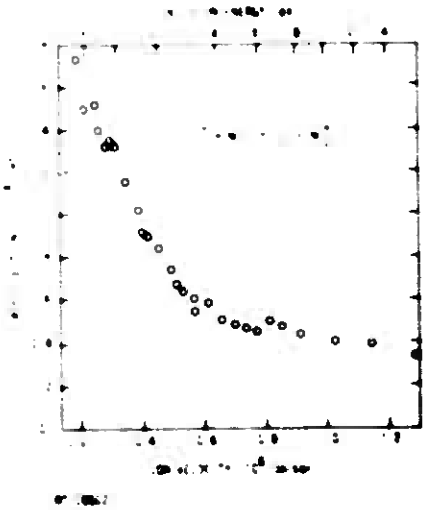

Figure 188 95 Cross section for the reaction $O_2^- + NO_2 \rightarrow O_2 + NO_2^-$ Circles are the data of Paulson (Reference 188 30) obtained using beam gas cell techniques

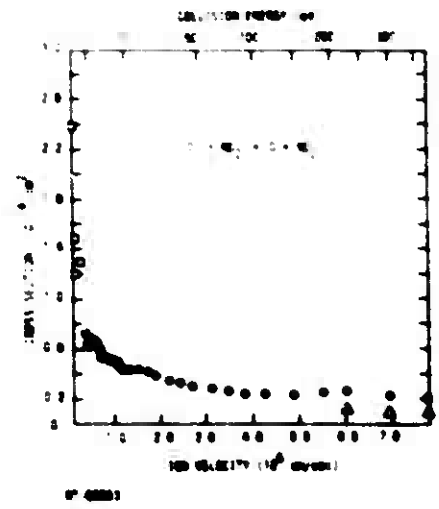

Figure 188 96 Cross section for the reaction $O^- + NO_2 \rightarrow O + NO_2^-$ Circles are the data of Rutherford (Reference 188 37) and triangles are the data of Snow, Rundel, and Gabelle (Reference 188 47) both obtained using crossed beam techniques Squares are the data of Stockdale, Compton and Reinhardt (Reference 188 52) obtained using ions produced by dissociative attachment

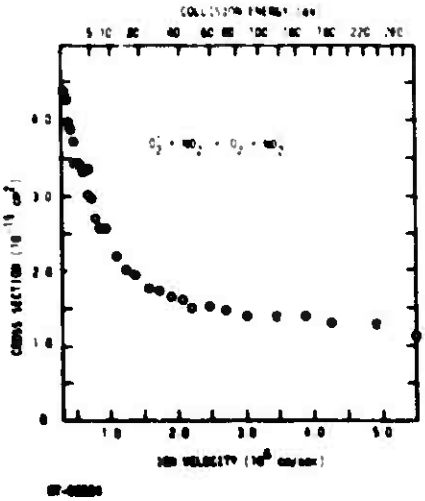

Figure 18B-97. Cross-section for the reaction $O_2^- + NO_2 \rightarrow O_2 + NO_2^-$. Circles are the data of Rutherford (Reference 18B-37) obtained using crossed-beam techniques.

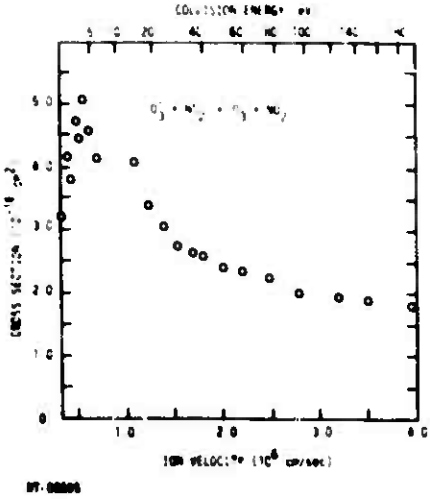

Figure 18B-98. Cross-section for the reaction $O_3^- + NO_2 \rightarrow O_3 + NO_2^-$. Circles are the data of Rutherford, Turner, and Vroom (Reference 18B-55) obtained using crossed-beam techniques.

18B.3.1.15 O_3-Molecule Reactions

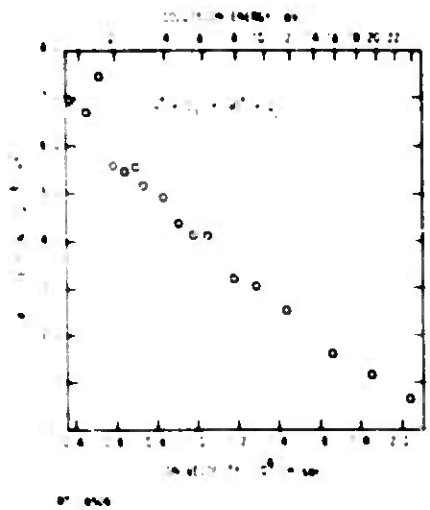

Figure 18B-99. Cross-section for the reaction $N^+ + O_3 \rightarrow NO^+ + O_2$. Circles are the data of Neynaber, Rutherford, and Vroom (Reference 18B-54) obtained using crossed-beam techniques.

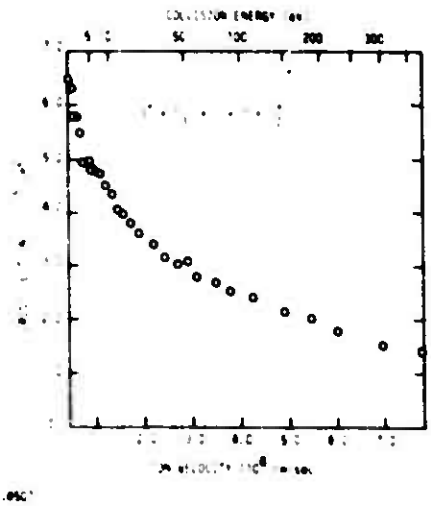

Figure 18B-100. Cross-section for the reaction $O^+ + O_3 \rightarrow O + O + O_2^+$. Circles are the data of Neynaber, Rutherford, and Vroom (Reference 18B-54) obtained using crossed-beam techniques.

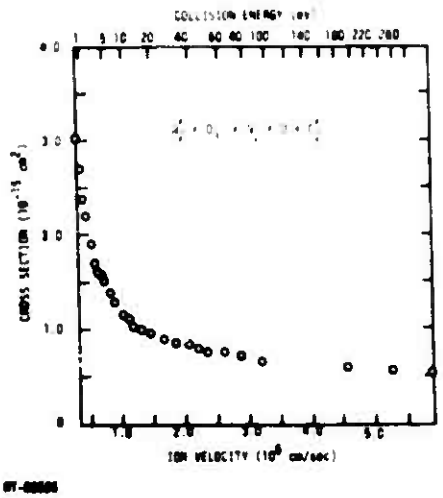

Figure 18B-101. Cross-section for the reaction $N_2^+ + O_3 \rightarrow N_2 + O + O_2^+$. Circles are the data of Naynaber, Rutherford, and Vroom (Reference 18B-54) obtained using crossed beam techniques.

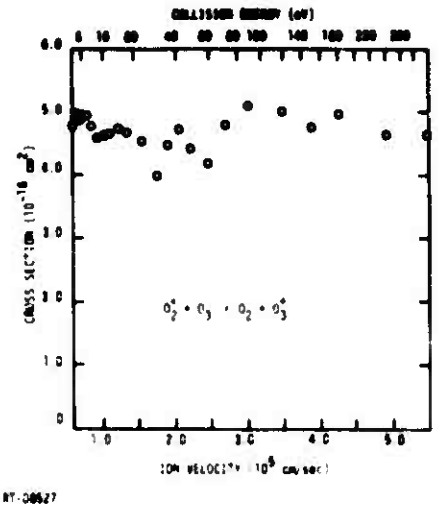

Figure 18B-102. Cross-section for the reaction $O_2^+ + O_3 \rightarrow O_2 + O_3^+$. Circles are the data of Neynaber, Rutherford, and Vroom (Reference 18B-54) obtained using crossed beam techniques.

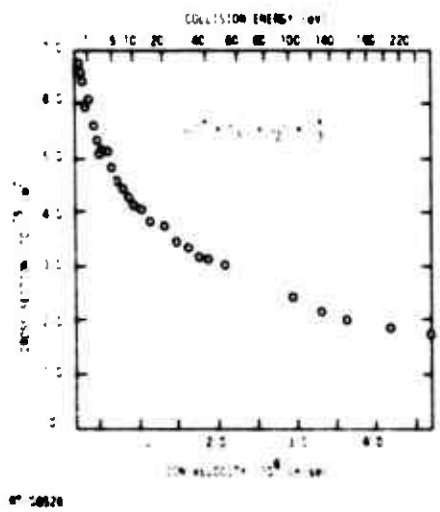

Figure 18B-103. Cross-section for the reaction $N_2O^+ + O_3 \rightarrow N_2O + O_3^+$. Circles are the data of Neynaber, Rutherford, and Vroom (Reference 18B-54) obtained using crossed-beam techniques.

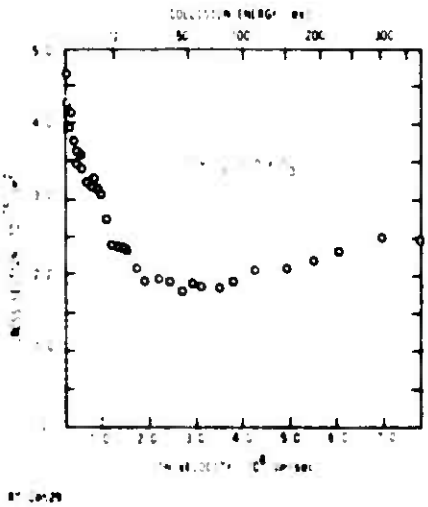

Figure 18B-104. Cross-section for the reaction $O^- + O_3 \rightarrow O + O_3^-$. Circles are the data of Rutherford, Turner, and Vroom (Reference 18B-55) obtained using crossed-beam techniques.

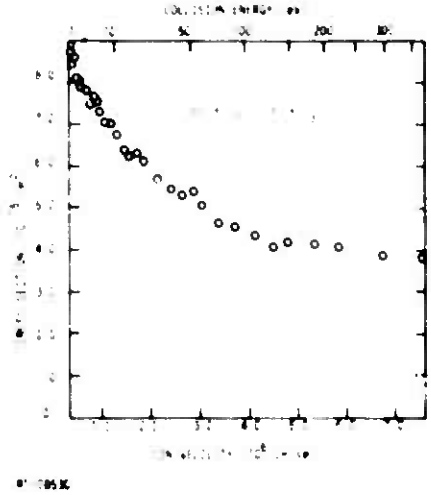

Figure 18B-105 Cross section for the reaction $OH^- + O_3 \rightarrow OH + O_3^-$. Circles are the data of Rutherford, Turner, and Vroom (Reference 18B-55) obtained using crossed-beam techniques.

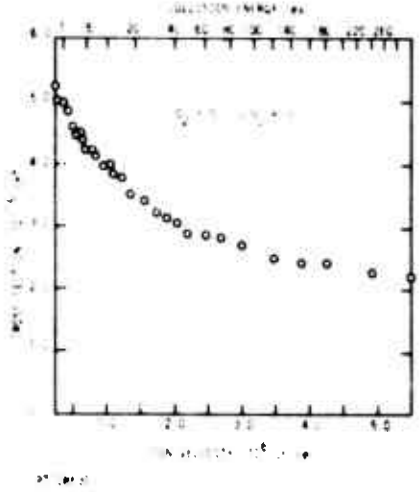

Figure 18B-106 Cross-section for the reaction $O_2^- + O_3 \rightarrow O_2 + O_3^-$. Circles are the data of Rutherford, Turner, and Vroom (Reference 18B-55) obtained using crossed-beam techniques.

18B.3.1.16 Drift-Tube and Flowing-Afterglow Drift-Tube Measurements

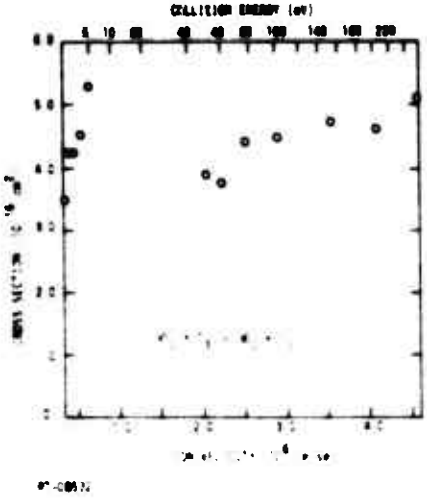

Figure 18B-107 Cross section for the reaction $NO_2^- + O_3 \rightarrow NO_2 + O_3^-$. Circles are the data of Rutherford, Turner, and Vroom (Reference 18B-55) obtained using crossed-beam techniques.

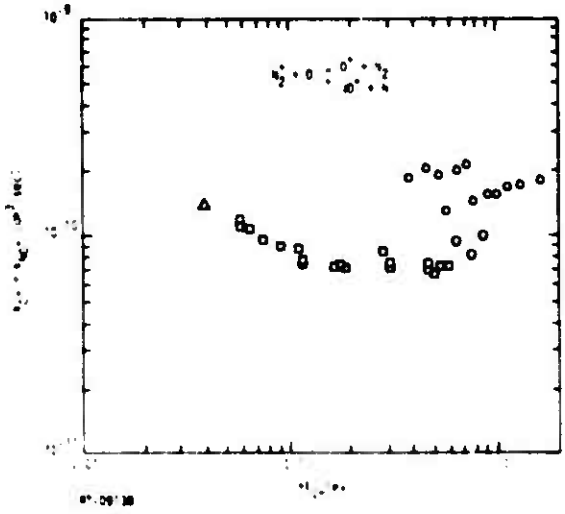

Figure 18B-108 Rate coefficients as a function of collision energy in the center-of-mass for the combined reactions $N_2^+ + O \rightarrow O^+ + N_2$ and $N_2^+ + O \rightarrow NO^+ + N$. Squares are the data of McFarland et al (Reference 18B-56) obtained using flowing-afterglow drift techniques, and the triangle is the thermal-energy datum of Fehsenfeld, Ounkin, and Ferguson (Reference 18B-57) obtained using afterglow techniques. Circles are the low-energy beam data of Rutherford and Vroom (Reference 18B-14) shown at higher energies for comparison.

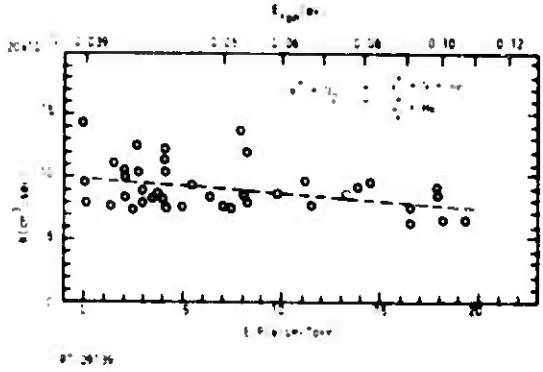

Figure 188-109. Rate coefficients as a function of E/P and of mean ion energy for the combined reactions $He^+ + N_2 \rightarrow N^+ + N + He$ (branching fraction 0.55) and $He^+ + N_2 \rightarrow N_2^+ + He$ (branching fraction 0.45). Circles are the data of Heimerl, Johnsen, and Biondi (Reference 188-12) obtained using drift-tube mass-spectrometer techniques.

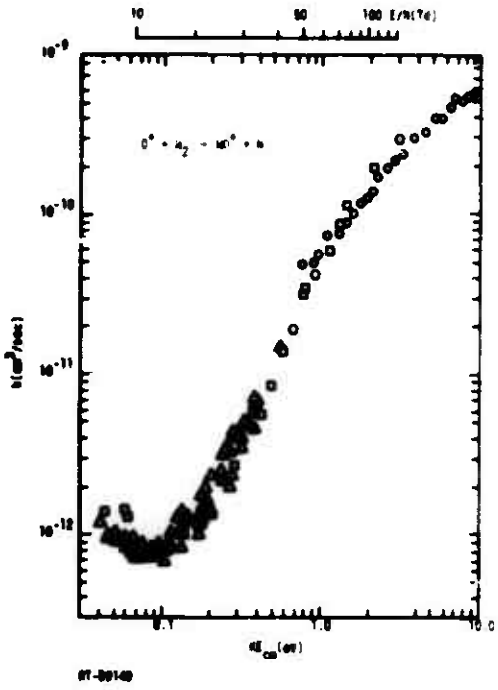

Figure 188 110. Rate coefficients as a function of the collision energy in the center-of-mass for the reaction $O^+ + N_2 \rightarrow NO^+ + N$. Squares are the data of McFarland et al (Reference 188-58) obtained using flowing-afterglow drift techniques and triangles are the data of Johnsen and Biondi (Reference 188-59) obtained using drift tube mass-spectrometer techniques. Circles are the beam data of Rutherford and Vroom (Reference 188-28) shown at higher energies for comparison.

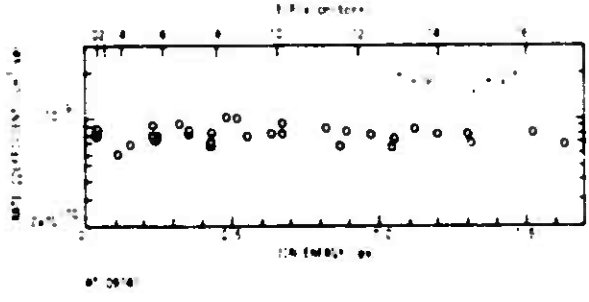

Figure 188-111. Rate coefficients as a function of E/P and of mean ion energy for the reaction $O_2^+ + NO \rightarrow O_2 + NO^+$. Circles are the data of Johnsen, Brown, and Biondi (Reference 188-60) obtained using drift tube mass-spectrometer techniques.

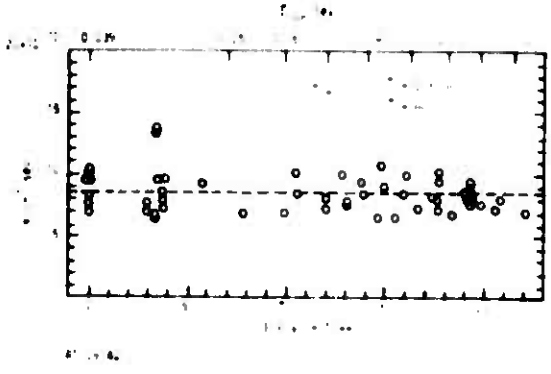

Figure 188 112. Rate coefficients as a function of E/P and of mean ion energy for the combined reactions $He^+ + O_2 \rightarrow O^+ + O + He$ (branching fraction 0.8) and $He^+ + O_2 \rightarrow O_2^+ + He$ (branching fraction 0.2). Circles are the data of Heimerl, Johnsen, and Biondi (Reference 188-12) obtained using drift tube mass-spectrometer techniques.

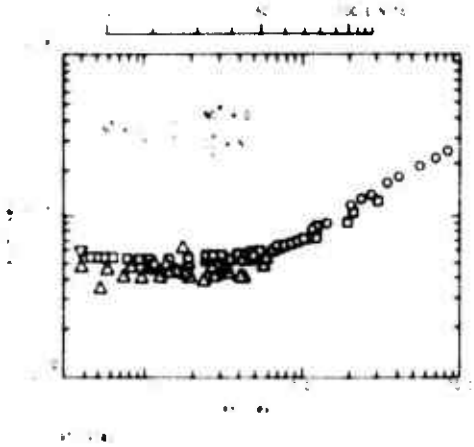

Figure 18B-113.

Rate coefficients as a function of the collision energy in the center-of-mass for the combined reactions $N^+ + O_2 \rightarrow NO^+ + O$ and $N^+ + O_2 \rightarrow O_2^+ + N$. Squares are the data of McFarland et al (Reference 18B-58) obtained using flowing-afterglow drift techniques, and triangles (apex up) are the data of Johnsen, Brown, and Biondi (Reference 18B-60) obtained using drift-tube mass-spectrometer techniques. The triangle (apex down) is the thermal-energy datum of Dunkin et al (Reference 18B-61) obtained using flowing-afterglow techniques, and circles are the beam data of Neynaber, Rutherford, and Vroom (Reference 18B-44) shown at higher energies for comparison.

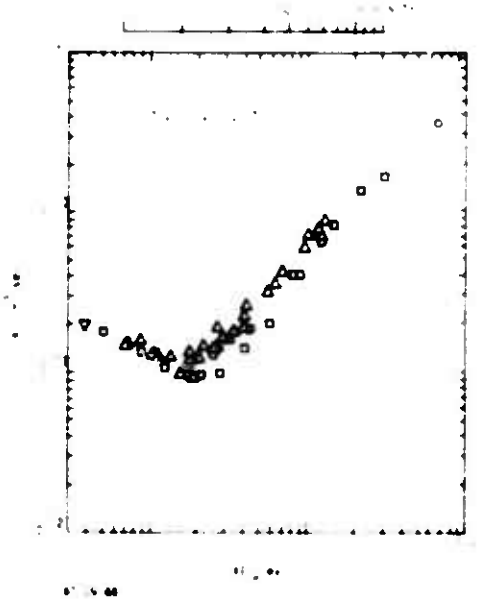

Figure 18B-114.

Rate coefficients as a function of the collision energy in the center of mass for the reaction $O^+ + O_2 \rightarrow O + O_2^+$. Squares are the data of McFarland et al (Reference 18B-58) obtained using flowing-afterglow drift techniques, and triangles (apex up) are the data of Johnsen and Biondi (Reference 18B-59) obtained using drift-tube mass-spectrometer techniques. The triangle (apex down) is the thermal-energy datum of Dunkin et al (Reference 18B-61) obtained using flowing-afterglow techniques, and the circle is a beam datum of Stebbings, Turner, and Rutherford (Reference 18B-5) shown here at higher energies for comparison.

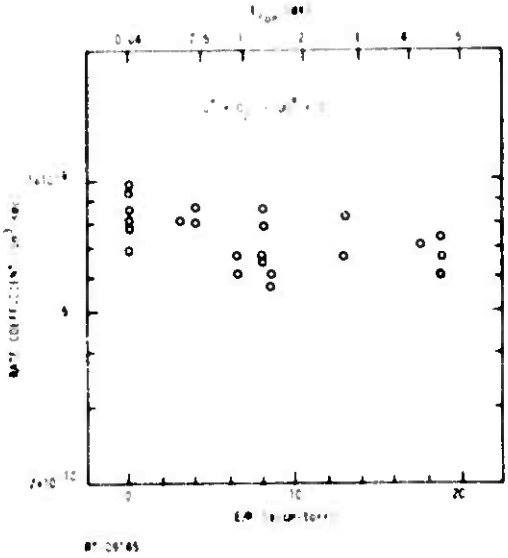

Figure 188-115. Rate coefficients as a function of E/P and of mean ion energy for the reaction $U^+ + O_2 \rightarrow UO^+ + O$. Circles are the data of Johnsen and Biondi (Reference 188-62) obtained using drift-tube mass-spectrometer techniques.

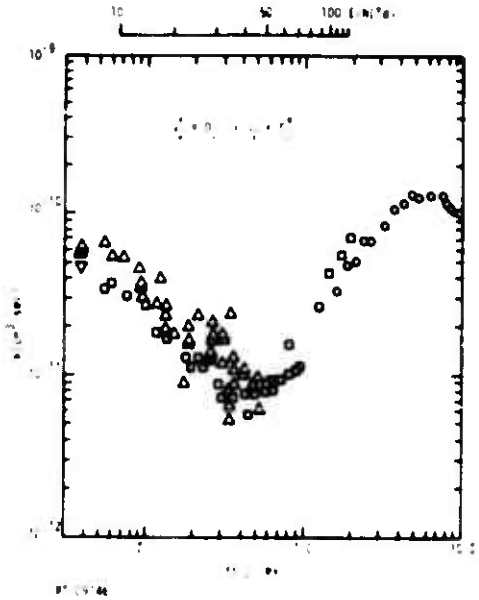

Figure 188-116. Rate coefficients as a function of the collision energy in the center-of-mass for the reaction $N_2^+ + O_2 \rightarrow N_2 + O_2^+$. Squares are the data of McFarland et al (Reference 188-58) obtained using flowing-afterglow drift techniques, and triangles (apex up) are the data of Johnsen, Brown, and Biondi (Reference 188-60) obtained using drift-tube mass-spectrometer techniques. The triangle (apex down) is the thermal-energy datum of Dunkin et al (Reference 188-61) obtained using flowing-afterglow techniques. Circles are the beam data of Neynaber, Rutherford, and Vroom (Reference 188-44) shown at higher energies for comparison.

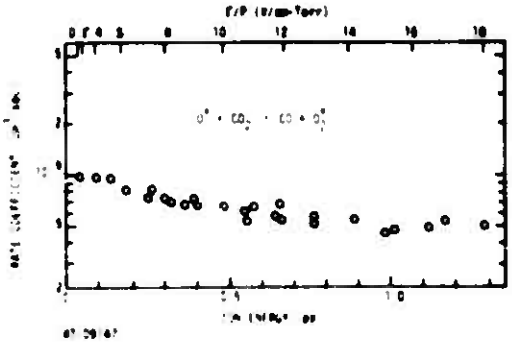

Figure 188-117. Rate coefficients as a function of E/P and of mean ion energy for the reaction $O^+ + CO_2 \rightarrow CO + O_2^+$. Circles are the data of Johnsen, Brown, and Biondi (Reference 188-60) obtained using drift-tube mass-spectrometer techniques.

18B.3.2 Tabular Data

Rate coefficients which have been measured at only one energy in the non-thermal energy regime are presented in Tables 18B-1 (positive-ion reactions) and 18B-2 (negative-ion reactions). It should be noted that all rates listed in these tables were determined using beam techniques. The ion energy employed was 0.5 eV. These compilations were prepared and kindly supplied to the chapter authors by L. O. Tiernan of Wright-Patterson Air Force Base, Ohio.

Table 18B-1. Rate coefficients for positive-ion reactions.

Reaction	Rate Coefficient** k (10^{-9} $cm^3 sec^{-1}$)	Reference
$^{14}N^+ + {}^{15}N_2 \rightarrow {}^{15}N^+ +$ neutral(s)	0.21	18B-29
$N_2^+ + {}^{15}N_2 \rightarrow N_2 + {}^{15}N_2^+$	0.67	18B-29
$O_2^{+*} + N_2 \rightarrow O_2 + N_2^+$	0.28	18B-29
$N^+ + {}^{15}NO \rightarrow N + {}^{15}NO^+$	0.093	18B-29
$O^+ + NO \rightarrow O + NO^+$	0.011	18B-63
$O^+ + N{}^{18}O \rightarrow {}^{18}O^+ +$ neutral(s)	0.091	18B-63
$O^+(^2D) + NO \rightarrow O + NO^+$	0.49	18B-29
$N_2^+ + NO \rightarrow N_2 + NO^+$	0.39	18B-29
$O_2^+ + NO \rightarrow O_2 + NO^+$	0.72	18B-29
$N^+ + O_2 \rightarrow N + O_2^+$	0.32	18B-64
$N^+ + O_2 \rightarrow NO^+ + O$	0.035	18B-64
$O^+ + O_2 \rightarrow O + O_2^+$	0.0057	18B-29
$O^+(^2D) + O_2 \rightarrow O + O_2^+$	0.59	18B-29
$N_2^+ + O_2 \rightarrow N_2 + O_2^+$	0.043	18B-64
$O_2^+ + {}^{18}O_2 \rightarrow O_2 + {}^{18}O_2^+$	0.60	18B-29

*Excited state.

**All rate coefficients are based upon normalization to 1.2×10^{-9} $cm^3 sec^{-1}$ for $CH_4^+ + CH_4 \rightarrow CH_5^+ + CH_3$.

(continued)

Table 18B-1 (Cont'd.)

Reaction	Rate Coefficient** k (10^{-9} $cm^3 sec^{-1}$)	Reference
$N^+ + H_2O \rightarrow N + H_2O^+$	0.65	18B-65
$N^+ + H_2O \rightarrow OH^+ + neutral(s)$	0.32	18B-65
$N^+ + H_2O \rightarrow HNO^+ + H$	0.038	18B-65
$O^+ + H_2{}^{18}O \rightarrow OH^+ + OH^*$	0.027	18B-65
$O^+ + H_2{}^{18}O \rightarrow O^{+*} + neutral(s)$	0.151	18B-65
$O^+ + H_2{}^{18}O \rightarrow O + H_2{}^{18}O^+$	1.13	18B-65
$N_2^+ + H_2O \rightarrow N_2 + H_2O^+$	0.61	18B-65
$N_2^+ + H_2O \rightarrow N_2H^+ + OH$	0.55	18B-65
$O_2^+ + H_2O \rightarrow O_2 + H_2O^+$	0.36	18B-65
$O_2^+ + H_2O \rightarrow HO_2^+ + OH$	0.14	18B-65
$O_2^+ + H_2O \rightarrow H_2O_2^+ + O$	0.043	18B-65
$O_2^+ + H_2O \rightarrow OH^+ + neutral(s)$	0.037	18B-65
$O^+ + N_2O \rightarrow N_2O^+ + O$	0.44	18B-29
$O^+(^2D) + N_2O \rightarrow N_2O^+ + O$	0.26	18B-29
$O^+(^2D) + N_2O \rightarrow NO^+ + N + O$	0.16	18B-29

*Excited state.

**All rate coefficients are based upon normalization to 1.2×10^{-9} $cm^3 sec^{-1}$ for $CH_4^+ + CH_4 \rightarrow CH_5^+ + CH_3$.

Table 18B-2. Rate coefficients for negative-ion reactions.

Reaction	Rate Coefficient** k (10^{-9} $cm^3 sec^{-1}$)	Reference
$CO_3^- + N_2 \rightarrow$ no reaction	<0.01	18B-29
$O_3^- + NO \rightarrow$ no reaction	<0.01	18B-29
$CO_3^- + NO \rightarrow$ no reaction	<0.01	18B-29
$NO^- + O_2 \rightarrow NO + O_2^-$	0.35	18B-66
$O_3^- + O_2 \rightarrow$ no reaction	<0.05	18B-29
$CO_3^- + O_2 \rightarrow$ no reaction	<0.01	18B-29
$O^- + H_2{}^{18}O \rightarrow OH^- + {}^{18}OH$	0.05	18B-66
$O^- + H_2{}^{18}O \rightarrow {}^{18}OH^- + OH$	0.05	18B-66
$NO_2^- + H_2O \rightarrow$ no reaction	<0.005	18B-29
$O^- + N_2{}^{18}O \rightarrow NO^- +$ neutral(s)	0.065	18B-29
$O^- + N_2{}^{18}O \rightarrow N{}^{18}O^- +$ neutral(s)	0.060	18B-38
$NO_2^- + N_2O \rightarrow$ no reaction	<0.005	18B-29
$O_3^- + CO_2 \rightarrow CO_3^- + O_2$	0.03	18B-29
$^{18}O^- + NO_2 \rightarrow {}^{18}O + NO_2^-$	1.08	18B-29

**All rate coefficients are based upon normalization to $1.0 \times 10^{-9} cm^3 sec^{-1}$ for $O^- + NO_2 \rightarrow O + NO_2^-$.

(continued)

Table 18B-2. (Cont'd.)

Reaction	Rate Coefficient** k (10^{-9} $cm^3 sec^{-1}$)	Reference
$O^- + NO_2 \rightarrow O^- + NO + O$	0.09	18B-66
$NO^- + NO_2 \rightarrow NO + NO_2^-$	0.23	18B-66
$O_2^- + NO_2 \rightarrow O_2 + NO_2^-$	0.76	18B-66
$O_3^- + NO_2 \rightarrow O_3 + NO_2^-$	0.22	18B-29
$CO_3^- + NO_2 \rightarrow$ no reaction	<0.01	18B-29
$O^- + O_3 \rightarrow O + O_3^-$	≥0.15	18B-29
$O_2^- + O_3 \rightarrow O_2 + O_3^-$	≥0.19	19B-29

**All rate coefficients are based upon normalization to $1.0 \times 10^{-9} cm^3 sec^{-1}$ for $O^- + NO_2 \rightarrow O + NO_2^-$.

REFERENCES

188-1. McFarland, M., D.L. Albritton, F.C. Fehsenfeld, E.E. Ferguson, and A.L. Schmeltekopf, J. Chem. Phys. 59, 6610 (1973).

188-2. Giese, C.F., and W.B. Maier, J. Chem. Phys. 39, 197 (1963).

188-3. Maier, W.B., J. Chem. Phys. 41, 2174 (1964).

188-4. Maier, W.B., J. Chem. Phys. 42, 1790 (1965).

188-5. Stebbings, R.F., B.R. Turner, and J.A. Rutherford, J. Geophys. Res. 71, 771 (1966).

188-6. Rutherford, J.A., R.F. Mathis, B.R. Turner, and D.A. Vroom, J. Chem. Phys. 55, 3788 (1971).

188-7. Paulson, J.F., F. Dale, and S.A. Studniarz, Intl. J. Mass Spectrom. ion Phys. 5, 115 (1970).

188-8. Seymour, R.H., in Advances in Atomic and Molecular Physics, D.R. Bates and I. Estermann, Eds., Academic Press, New York (1969); Vol. 5, p. 57.

188-9. Dunn, G.H., in Atomic Physics, B. Bederson, V.W. Cohen, and F.M.J. Pichanick, Eds., Plenum Press, New York (1969); p. 417.

188-10. Lampe, F.W., J.L. Franklin, and F.H. Field, in Progress in Reaction Kinetics, G. Porter, Ed., Pergamon Press, New York (1961); Vol. 1, p. 67.

188-11. Albritton, D.L., T.M. Miller, D.W. Martin, and E.W. McDaniel, Phys. Rev. 171, 94 (1968).

188-12. Heimerl, J.M., R. Johnsen, and M.A. Biondi, J. Chem. Phys. 51, 5041 (1969).

188-13. Kaneko, Y., T.R. Megill, and J.F. Hasted, J. Chem. Phys. 46, 4731 (1967).

188-14. Rutherford, J.A., and D.A. Vroom, J. Chem. Phys. 61, 2514 (1974).

188-15. Stebbings, R.F., A.C.H. Smith, and H. Ehrhardt, J. Geophys. Res. 69, 2349 (1964).

188-16. Rutherford, J.A., R.F. Mathis, B.R. Turner, and D.A. Vroom, J. Chem. Phys. 57, 4578 (1972).

18B-17. Peterson, J.R., and D.C. Lorents, Phys. Rev. 182, 152 (1969).

18B-18. Rutherford, J.A., R.F. Mathis, B.R. Turner, and D.A. Vroom, J. Chem. Phys. 57, 3087 (1972).

18B-19. Rutherford, J.A., and D.A. Vroom, J. Chem. Phys. 57, 3091 (1972).

18B-20. Neynaber, R.H., G.D. Magnuson, S.M. Trujillo, and B.F. Myers, Phys. Rev. A5, 285 (1972).

18B-21. Maier, W.B., Planet. Space Sci. 16, 477 (1968).

18B-22. Stebbings, R.F., J.A. Rutherford, and B.R. Turner, Planet. Space Sci. 13, 1125 (1965).

18B-23. Gustafsson, E., and E. Lindholm, Ark. Fys. 18, 219 (1960).

18B-24. Moran, T.F., and L. Friedman, J. Chem. Phys. 45, 3837 (1966).

18B-25. Maier, W.B., and E. Murad, J. Chem. Phys. 55, 2307 (1971).

18B-26. Neynaber, R.H., J.A. Rutherford, and D.A. Vroom, Gulf Radiation Technology Report Gulf-RT-A10767 (1971).

18B-27. Stebbings, R.F., B.R. Turner, and A.C.H. Smith, J. Chem. Phys. 38, 2277 (1963).

18B-28. Rutherford, J.A., and D.A. Vroom, J. Chem. Phys. 55, 5622 (1971).

18B-29. Tiernan, T.O., private communication (1974).

18B-30. Paulson, J.F., unpublished data.

18B-31. Giese, C.F., in Ion Molecule Reactions in the Gas Phase, R.F. Gould, Ed., Advances in Chemistry Series, Vol. 58, Am. Chem. Soc., Washington (1966); p. 20.

18B-32. Moran, T.F., and J.R. Roberts, J. Chem. Phys. 49, 3411 (1968).

18B-33. Yeff, S.H., Astrophys. J. 140, 348 (1964).

18B-34. Leventhal, J.J., T.F. Moran, and L. Friedman, J. Chem. Phys. 46, 4666 (1967).

189-35. Amme, R.C., and [illegible], in Atomic Collision Processes, M.R.C. McDowell, Ed., North Holland Publishing Co., Amsterdam (1964), p. 847.

189-36. Maier, W.B., J. Chem. Phys. [illegible], [illegible] (1971).

189-37. Rutherford, J.A., unpublished data.

189-38. [illegible], and [illegible] Chow, in Advances in Mass Spectrometry, A.R. West, Ed., Applied Science Publishers, Ltd., Barking, Essex, England (1974), Vol. [illegible], p. [illegible].

189-39. [illegible], J.A. Rutherford, and [illegible] Stebbings, J. Geophys. Res. [illegible] (1969).

189-40. [illegible], and [illegible] Sheridan, J. Chem. Phys. 27, [illegible] (1957).

189-41. [illegible], and [illegible] Rutherford, J. Geophys. Res. [illegible] (1969).

189-42. [illegible], [illegible] Smith, [illegible] Stebbings, and [illegible] Rutherford, [illegible] Res. [illegible], 2022 (1969).

189-43. [illegible] unpublished data.

189-44. [illegible] Rutherford, and [illegible] [illegible]

189-45. [illegible]

189-46. [illegible]

189-47. [illegible]

189-48. [illegible]

189-49. [illegible]

18B-53. Paulson, J.F., J. Chem. Phys. 52, 963 (1970).

18B-54. Neynaber, R.H., J.K. Layton, J.A. Rutherford, and D.A. Vroom, Gulf Radiation Technology Report GA-10286 (1970).

18B-55. Rutherford, J.A. B.R. Turner, and D.A. Vroom, J.Chem. Phys. 58, 5267 (1973).

18B-56. McFarland, M., D.L. Albritton, F.C. Fehsenfeld, E.E. Ferguson, and A.L. Schmeltekopf, J. Geophys. Res. 79, 2925 (1974).

18B-57. Fehsenfeld, F.C., D.B. Dunkin, and E.E. Ferguson, Planet. Space Sci. 18, 1267 (1970).

18B-58. McFarland, M., D.L. Albritton, F.C. Fehsenfeld, E.E. Ferguson, and A.L. Schmeltekopf, J. Chem. Phys. 59, 6620 (1973).

18B-59. Johnsen, R., and M.A. Biondi, J. Chem. Phys. 59, 3504 (1973).

18B-60. Johnsen, R., H.L. Brown, and M.A. Biondi, J. Chem. Phys. 52, 5080 (1970).

18B-61. Dunkin, D.B., F.C. Fehsenfeld, A.L. Schmeltekopf, and E.E. Ferguson, J. Chem. Phys. 49, 1365 (1968).

18B-62. Johnsen, R., and M.A. Biondi, J. Chem. Phys. 57, 1475 (1972).

18B-63. Hughes, B.M., and T.C. Tiernan, DASA Symposium on the Physics and Chemistry of the Upper Atmosphere, Philadelphia (1970).

18B-64. Tiernan, T.C., and B.M. Hughes, 18th Annual Conference on Mass Spectrometry and Allied Topics, San Francisco (1970).

18B-65. Tiernan, T.C., and B.M. Hughes, DASA Symposium on the Physics and Chemistry of the Upper Atmosphere, Stanford Research Institute (1969).

18B-66. Tiernan, T.C., and B.M. Hughes, Proceedings of the CAR Research Applications Conference (CAR 69-0011, AD 692500), Arlington, Va. (1969).

THIS PAGE IS INTENTIONALLY LEFT BLANK.